

# Journal of Geophysical Research Earth Surface

The *JGR* editors welcome original scientific contributions on the physics and chemistry of the Earth, its environment, and the solar system.

*JGR-Earth Surface* focuses on the physical, chemical, and biological processes that affect the form and function of the surface of the solid Earth over all temporal and spatial scales, including fluvial, eolian, and coastal sediment transport; hillslope mass movements; glacial and periglacial activity; weathering and pedogenesis; and surface manifestations of volcanism and tectonism.

Please submit your manuscript electronically by logging on to <http://jgr-earthsurface-submit.agu.org>, and following the instructions. For the peer-review process you may submit text in Microsoft Word, LaTeX, or PDF; artwork should be submitted as encapsulated postscript (.eps), tagged information file format (.tif), .jpg, or .pdf files. See <http://publications.agu.org/author-resource-center/author-guide/> for information about file preparation. For production, PDFs are not acceptable.

## Editors

Alexander L. Densmore, Editor in Chief  
Institute of Hazard, Risk and Resilience  
and Department of Geography  
Durham University  
Durham, United Kingdom

Bryn Hubbard  
Centre for Glaciology  
Institute of Geography and Earth Sciences  
Aberystwyth University  
Ceredigion, United Kingdom

Submit papers to <http://jgr-earthsurface-submit.agu.org/>

## AGU Editorial Team Senior Journal Program Manager

Randy Townsend  
[earthsurface@agu.org](mailto:earthsurface@agu.org)

## Associate Editors

Sridhar Anandakrishnan	Dmitri Lague
Andrew Ashton	Stephen Lancaster
Jeremy Bassis	Bruce MacVicar
Mike Bentley	Jon J. Major
Simon Brocklehurst	Simon Mudd
John Buffington	John Pitlick
Poul Christoffersen	Duncan Quincey
Giovanni Cocco	Colin David Rennie
Emmanuel Gabet	Martin Schneebeli
Nicole Gasparini	Douglas Sherman
Kimberly Hill	Martin Truffer
Wonsuck Kim	Tingjun Zhang

Brooks Hanson, Director of Publications  
Victoria Forlini, Assistant Director of Editor Support

*Journal of Geophysical Research: Earth Surface* (ISSN 2169-9003, print; ISSN 2169-9011, online) is published quarterly in March, June, September, and December on behalf of the American Geophysical Union by Wiley Subscription Services, Inc., a Wiley Company, 111 River St., Hoboken NJ 07030-5774. Postmaster: Send all address changes to *Journal of Geophysical Research: Earth Surface*, John Wiley & Sons Inc., C/O The Sheridan Press, PO Box 465, Hanover, PA 17331.

**Manuscript Submission:** Articles should be submitted to the appropriate journal using GEMS. There is a submission link on each journal homepage on the Wiley Online Library web site.

Through electronic submissions the corresponding author affirms that (1) all authors listed on manuscripts are aware of the submission to this journal and (2) this manuscript has not been published previously nor is under consideration by another journal. It is unethical for an author to publish manuscripts describing essentially the same research in more than one journal of primary publication. Submitting the same manuscript to more than one journal concurrently is unethical and unacceptable.

**Final File Formats.** For the final accepted article you may submit text in Microsoft Word or LaTeX; final artwork should be submitted as encapsulated postscript (.eps), tagged information file format (.tif), .jpg, or .pdf files. See <http://publications.agu.org/author-resource-center/author-guide/> for information about file preparation.

**Publication Charges.** The publication charge income received for *JGR-Earth Surface* helps support rapid publication, allows more articles per volume, makes possible the low subscription rates, and supports many of AGU's scientific and outreach activities. Publication charge information can be found here: <http://publications.agu.org/author-resource-center/author-guide/publication-fees/>.

To encourage papers to be written in a concise fashion, there is an excess length fee. For *JGR-Earth Surface* the fee is assessed only on the equivalent of more than 25 publication units. The excess length fee does not apply to review articles, and the editor may waive the fee on a limited number of concisely written papers that merit being longer. There is no charge for color in any format.

**Subscriptions.** AGU members may subscribe to the *JGR-Earth Surface* online editions for their personal use. The annual rate for access to the online edition is \$50. Student members may subscribe at reduced rates. Contact AGU for individual section rates and for special rates for libraries and other multiple-use institutions. Individual issues are offered for sale based on availability; please contact Member Services with such requests.

**Supporting Information.** Supporting information may be in the form of data tables, figures, videos, or software applications. Please refer to <http://publications.agu.org/author-resource-center/author-guide/text-requirements/#supmat> for additional information about acceptable file formats and sizes. Such material will be subjected to the same peer review procedures used for articles.

**Claims and Changes of Address.** Send address changes to the AGU Member Service Center with at least 5 weeks' advance notice. Claims for missing issues due to insufficient notice of address change or such reasons as "missing from files" cannot be serviced.

**Copyright.** Permission is granted for individuals to make single copies for personal use in research, study, or teaching and to use figures, tables, and short quotes from this journal for republication in scientific books and journals. There is no charge for any of these uses, but the material must be cited appropriately. The appearance of the code at the bottom of the first page of an article in this journal indicates the copyright owner's consent that copies of the article may be made for personal or internal use or for the personal or internal use of specific clients. This consent is given on the condition that the copier pay the stated per copy fee through the Copyright Clearance Center, Inc., for copying beyond that permitted by Section 107 or Section 108 of the U.S. Copyright Law. This consent does not extend to other kinds of copying, such as copying for general distribution, for advertising or promotional purposes, for creating new collective works, or for resale. Articles published prior to 1980 are subject to the same provisions. The reproduction of multiple copies, the use of full articles, or the use of extracts for commercial purposes requires special permission from AGU.

Address all correspondence to the appropriate department at AGU, 2000 Florida Avenue, N.W., Washington, DC 20009 USA.

**AGU Headquarters.** The AGU Member Service Center is open from 8:00 a.m. to 6:00 p.m. Eastern time to take calls of a general nature related to membership, subscriptions, and meetings: +1 202.462.6900, +1 800.966.2481; fax: +1 202.328.0566; e-mail: [service@agu.org](mailto:service@agu.org).

Questions of a specific nature will be referred to appropriate staff. The following e-mail addresses and direct dial lines to the publications department are provided to expedite information relative to article status, reprints, and publication fees.

For assistance with submitted manuscripts, file specifications, or AGU publication policy, please contact the journal home office: [jgr-EarthSurface@agu.org](mailto:jgr-EarthSurface@agu.org). For assistance with post-acceptance articles, reprints, or other production issues, please contact Wiley production: [JGRFprod@wiley.com](mailto:JGRFprod@wiley.com).

View this journal online at [wileyonlinelibrary.com/journal/JGRF](http://wileyonlinelibrary.com/journal/JGRF).

The online article is the official version and may contain additional content not available in this print issue. To access the full article, including multimedia, enhanced figures, supporting information, and other nonprinted content, go to <http://wileyonlinelibrary.com/journal/jgrf>.

## Research Articles

- 1783** *J. Gaume, J. Schweizer, A. van Herwijnen, G. Chambon, B. Reuter, N. Eckert, and M. Naaim*  
Evaluation of slope stability with respect to snowpack spatial variability  
(doi 10.1002/2014JF003193)
- 1800** *Lizeth Caballero, Damiano Sarocchi, Enrique Soto, and Lorenzo Borselli*  
Rheological changes induced by clast fragmentation in debris flows (doi 10.1002/2013JF002942)
- 1818** *A. Pelosi, G. Parker, R. Schumer, and H.-B. Ma*  
Exner-Based Master Equation for transport and dispersion of river pebble tracers: Derivation, asymptotic forms, and quantification of nonlocal vertical dispersion (doi 10.1002/2014JF003130)
- 1833** *Lindsey K. Albertson, Leonard S. Sklar, Patricia Pontau, Michelle Dow, and Bradley J. Cardinale*  
A mechanistic model linking insect (Hydropsychidae) silk nets to incipient sediment motion in gravel-bedded streams  
(doi 10.1002/2013JF003024)
- 1853** *Matthew Fox, Liran Goren, Dave A. May, and Sean D. Willett*  
Inversion of fluvial channels for paleorock uplift rates in Taiwan (doi 10.1002/2014JF003196)
- 1876** *A. Gilbert, O. Gagliardini, C. Vincent, and P. Wagnon*  
A 3-D thermal regime model suitable for cold accumulation zones of polythermal mountain glaciers  
(doi 10.1002/2014JF003199)
- 1894** *Mauro Perego, Stephen Price, and Georg Stadler*  
Optimal initial conditions for coupling ice sheet models to Earth system models (doi 10.1002/2014JF003181)
- 1918** *E. Larour, A. Khazendar, C. P. Borstad, H. Seroussi, M. Morlighem, and E. Rignot*  
Representation of sharp rifts and faults mechanics in modeling ice shelf flow dynamics: Application to Brunt/Stancomb-Wills Ice Shelf, Antarctica (doi 10.1002/2014JF003157)
- 1936** *Kristen D. Splinter, Ian L. Turner, Mark A. Davidson, Patrick Barnard, Bruno Castelle, and Joan Oltman-Shay*  
A generalized equilibrium model for predicting daily to interannual shoreline response  
(doi 10.1002/2014JF003106)
- 1959** *Jeremy G. Venditti and Michael Church*  
Morphology and controls on the position of a gravel-sand transition: Fraser River, British Columbia  
(doi 10.1002/2014JF003147)
- 1977** *Sagar Prasad Parajuli, Zong-Liang Yang, and Gary Kocurek*  
Mapping erodibility in dust source regions based on geomorphology, meteorology, and remote sensing  
(doi 10.1002/2014JF003095)
- 1995** *Richard M. Morris, Douglas W. F. Mair, Peter W. Nienow, Christina Bell, David O. Burgess, and Andrew P. Wright*  
Field-calibrated model of melt, refreezing, and run off for polar ice caps: Application to Devon Ice Cap  
(doi 10.1002/2014JF003100)

- 2013** *David Walters, Laura J. Moore, Orencio Duran Vinent, Sergio Fagherazzi, and Giulio Mariotti*  
Interactions between barrier islands and backbarrier marshes affect island system response to sea level rise: Insights from a coupled model (doi 10.1002/2014JF003091)
- 2032** *S. V. Kokelj, T. C. Lantz, S. A. Wolfe, J. C. Kanigan, P. D. Morse, R. Coutts, N. Molina-Giraldo, and C. R. Burn*  
Distribution and activity of ice wedges across the forest-tundra transition, western Arctic Canada (doi 10.1002/2014JF003085)
- 2048** *Dylan J. Ward and Joseph Galewsky*  
Exploring landscape sensitivity to the Pacific Trade Wind Inversion on the subsiding island of Hawaii (doi 10.1002/2014JF003155)
- 2070** *J. Peakall, S. E. Darby, R. M. Dorrell, D. R. Parsons, E. J. Sumner, and R. B. Wynn*  
Comment on "A simple model for vertical profiles of velocity and suspended sediment concentration in straight and curved submarine channels" by M. Bolla Pittaluga and J. Imran (doi 10.1002/2014JF003211)
- 2074** *M. Bolla Pittaluga, J. Imran, D. Medicina, and G. Parker*  
Reply to comment by J. Peakall et al. on "A simple model for vertical profiles of velocity and suspended sediment concentration in straight and curved submarine channels" (doi 10.1002/2014JF003273)

---

**Cover.** In *Venditti and Church* [DOI: 10.1002/2014JF003147], image shows sedimentology of Hatzic Bar. (a) Gravel surface veneer on head of bar, (b) sand-gravel mixture immediately below the gravel surface veneer, and (c) subsurface material in trench ~30 cm deep at location i (bar head). (d) Gravel-sand mixture downstream of the bar head at location ii (downstream of bar head). (e) View downstream of location ii looking toward location iii (midbar) showing the transition from a gravel-sand mix to a sand surface. (f) Sand surface with patches of finer silt-clay (in bed form troughs) on the bar tail at location iv. (g) Grain-size distributions of samples collected along a north-west transect along Hatzic Bar. Bed topography and tricolor grain-size bars are the same as in Figure 7c. Distributions labeled "crest" and "trough" refer to positions over low amplitude, symmetric, sand dunes developed on the bar with coarser crests and finer troughs. Distributions labeled "bulk" are where there was no obvious surface coarsening with respect to the subsurface. See pp. 1959–1976.

## RESEARCH ARTICLE

10.1002/2014JF003147

## Key Points:

- Gravel-sand transitions terminate as a gravel wedge with a diffuse extension
- GST due to decline in gravel mobility and sand deposition from suspension
- Change in shear stress in GST is a consequential feature of the transition

## Correspondence to:

J. G. Venditti,  
jeremy\_venditti@sfu.ca

## Citation:

Venditti, J. G., and M. Church (2014), Morphology and controls on the position of a gravel-sand transition: Fraser River, British Columbia, *J. Geophys. Res. Earth Surf.*, 119, 1959–1976, doi:10.1002/2014JF003147.

Received 13 MAR 2014

Accepted 22 AUG 2014

Accepted article online 27 AUG 2014

Published online 23 SEP 2014

## Morphology and controls on the position of a gravel-sand transition: Fraser River, British Columbia

Jeremy G. Venditti<sup>1</sup> and Michael Church<sup>2</sup>

<sup>1</sup>Department of Geography, Simon Fraser University, Burnaby, British Columbia, Canada, <sup>2</sup>Department of Geography, The University of British Columbia, Vancouver, British Columbia, Canada

**Abstract** Alluvial river channels often exhibit a relatively abrupt transition from gravel- to sand-bedded conditions. The phenomenon is well documented, but few prior studies have analyzed the spatial variability through reaches where transitions occur. The downstream fining pattern observed in the Fraser River is cited as a classic example of an abrupt gravel-sand transition in a large alluvial channel. However, important questions regarding the exact location of the transition, its sedimentology and morphology, and what controls its location remain unanswered. Here we present observations of the downstream change in bed material grain size, river bed topography, and channel hydraulics through the reach within which the transition occurs. These observations indicate that the gravel-sand transition is characterized by a terminating gravel wedge, but there are patches of gravel downstream of the wedge forming a diffuse extension. We show that there is a dramatic decrease in shear stress at the downstream end of the wedge and a consequent cessation of general gravel mobility. We argue that the patches of gravel observed beyond the wedge are the result of enhanced mobility of fine gravel over a sand bed. We also find that sand in suspension declines rapidly at the downstream end of the wedge, suggesting that sand is delivered to the bed, completing the sedimentary conditions for a gravel-sand transition. We propose that the break in river slope associated with the transition is a consequential feature of the transition.

### 1. Introduction

Bed sediments in alluvial river channels generally become finer downstream. It is widely accepted that bed material size declines exponentially with distance downstream in the absence of lateral sediment inputs [e.g., Sternberg, 1875; Yatsu, 1955; Church and Kellerhals, 1978; Rice and Church, 1998]. In many channels, a significant discontinuity in the bed material grain size fining trend occurs over a relatively short downstream distance where the bed material changes from gravel to sand [Yatsu, 1957; Howard, 1980; Shaw and Kellerhals, 1982; Brierley and Hickin, 1985; Sambrook Smith and Ferguson, 1995; Dade and Friend, 1998; Knighton, 1999; Ferguson, 2003; Gran et al., 2006; Singer, 2008, 2010; Ferguson et al., 2011; Frings, 2011; Labbe et al., 2011]. Through the short intervening reach, bed material is a bimodal mixture of sand and gravel [Sambrook Smith and Ferguson, 1995; Ferguson et al., 2011].

Superficially, the gravel-sand transition is a change from a gravel bed channel to a sand bed one, but this may happen at a variety of scales in rivers, ranging from the long profile to bar or bed form scale transitions. It may also occur due to seasonal loading of sand to a channel [e.g., Gran et al., 2006; Gran, 2012] or secular changes in sediment supply associated with land use change and river regulation [e.g., Singer, 2008, 2010]. More informatively, the gravel-sand transition has been associated with an abrupt increase in the sand fraction of the bed material to values in excess of 20% [Wilcock, 1998; Frings, 2011] when the deposit becomes matrix supported. For such quantities of sand to remain present in the bed, shear stresses must decline to values that prevent their onward movement in suspension. Such stress values also limit the mobility of larger clasts, hence the cessation of general gravel movement. This causes a discontinuity in the size of the bed material, which is sometimes also reflected in the channel morphology [Labbe et al., 2011] and can be distinguished from sand pulses moving through a river system. Gravel may nevertheless be carried beyond this point by being rafted over the emerging, smoother sand bed [Wilcock et al., 2001], accounting for a diffuse continuation of gravel beyond the onset point of the transition. In the field, details of channel morphology and hydraulics create a range of sand content values through the transition, varying from 20% to 30% at the inception of the transition [Wilcock, 1998; Wilcock et al., 2001; Ferguson, 2003; Frings, 2011] to 50–75% at the end of the transition [Sambrook Smith and Ferguson, 1995; Frings, 2011].

Several mechanisms have been proposed for the emergence of a gravel-sand transition, including the following: (1) the disintegration of fine gravel particles of certain lithologies into sand-sized mineral grains during the transport process [cf. *Yatsu, 1957; Kodama, 1994*] or rock weathering [*Wolcott, 1988*] and the consequent existence of a grain size gap between 1 and 10 mm, (2) selective transport caused by a decline in the capacity of the river to carry larger particles [cf. *Brierley and Hickin, 1985; Ferguson et al., 1996, 1998; Wilcock, 1998; Ferguson, 2003; Ferguson et al., 2011; Frings, 2011*], and (3) external base-level control that generates a backwater effect and a rapid decline in transport capacity [cf. *Pickup, 1984; Sambrook Smith and Ferguson, 1995*]. What these mechanisms have in common is a general cessation of transport by the river of grain sizes coarser than sand.

In spite of the variety of candidate explanations for the gravel-sand transition, there remains a paucity of detailed studies of grain size change through these transitions, particularly in large channels where details of the phenomenon are apt to be best revealed. Indeed, most of the detailed studies of grain size change have focused on small upland streams with widths on the order of meters and depths on the order of tens of centimeters [*Sambrook Smith and Ferguson, 1996; Ferguson et al., 1996, 1998*] or even smaller laboratory flumes [*Paola et al., 1992; Wilcock, 1998*]. Fewer studies have focused on the gravel-sand transition in larger alluvial channels with widths on the order of tens to hundreds of meters and flow depths of order meters to tens of meters, although gravel-sand transitions certainly have been studied in larger channels [cf. *Yatsu, 1955, 1957; McLean et al., 1999; Singer, 2008, 2010; Frings, 2011*].

Investigations in small channels and flumes have suggested that the gravel-sand transition is abrupt and characterized by a so-called “arrested” gravel front [cf. *Paola et al., 1992; Sambrook Smith and Ferguson, 1995*]. However, *Ferguson et al.* [2011] observed a nonabrupt transition in a 50 m wide channel, though the total distance for the transition remained relatively short at ~3 km (60 channel widths); *Frings* [2011] reported that the transition in the River Rhine occurs over a reach of order 100 channel widths, and *Singer* [2008, 2010] reported a contemporary transition that occurs over 175 km (~1500 channel widths) in the Sacramento River, California. Aside from these cases, sampling in larger channels remains too sparse to assess the abruptness of the transition or to draw conclusions as to its cause. The morphology, abruptness, and occurrence of gravel-sand transitions remain an open problem because larger-scale channels can accommodate changes in bed material supply from upstream or tributaries through lateral variability in grain size [cf. *Frings, 2011*] that is generally not possible in small channels or flumes. Also, the role that the variability in bed topography plays in the transition cannot be assessed in small channels or flumes, where topographic variability and the range of sedimentary environments are limited. *Singer* [2008, 2010] speculated that the diffuse nature of the transition in the Sacramento River is a transitory response to secular reduction in sediment supply to the system that entails the transition ultimately moving of order 100 km upstream. This case challenges the idea of the gravel-sand transition occurring at the point of cessation of downstream gravel transport.

Fraser River in British Columbia (BC) appears to represent an archetypical example of a gravel-sand transition in a large channel [*Sambrook Smith and Ferguson, 1995; McLean et al., 1999; Kleinhans, 2002*]. The river remains largely unmodified by human action. One headwater, comprising less than 2% of the total drainage area, is regulated, and sedimentary disturbance far upriver occurred in the form of nineteenth century placer mining. There is no evidence, however, that the effect of that history has disturbed sedimentary processes at the distal limit of gravel accumulation. Here we report on observations of the downstream change in bed material composition and channel hydraulics in the alluvial reach of the lower Fraser River, including a bed sampling program undertaken to pinpoint the location of the gravel-sand transition. We seek answers to the following questions: (1) Where is the gravel-sand transition and what is its morphology? (2) How does gravel mobility change across the gravel-sand transition? (3) What controls the location of the gravel-sand transition?

## 2. Field Site

Fraser River drains 228,000 km<sup>2</sup> of southwestern BC. The headwaters of the river are near Mount Robson along the British Columbia-Alberta border, whence it flows 1375 km into the Strait of Georgia at Sand Heads (Figure 1a). Approximately 486 km from the sea at the confluence with the Chilcotin River, the Fraser enters a series of bedrock canyons that funnel sediment from the BC interior plateau and mountains to the distal reaches

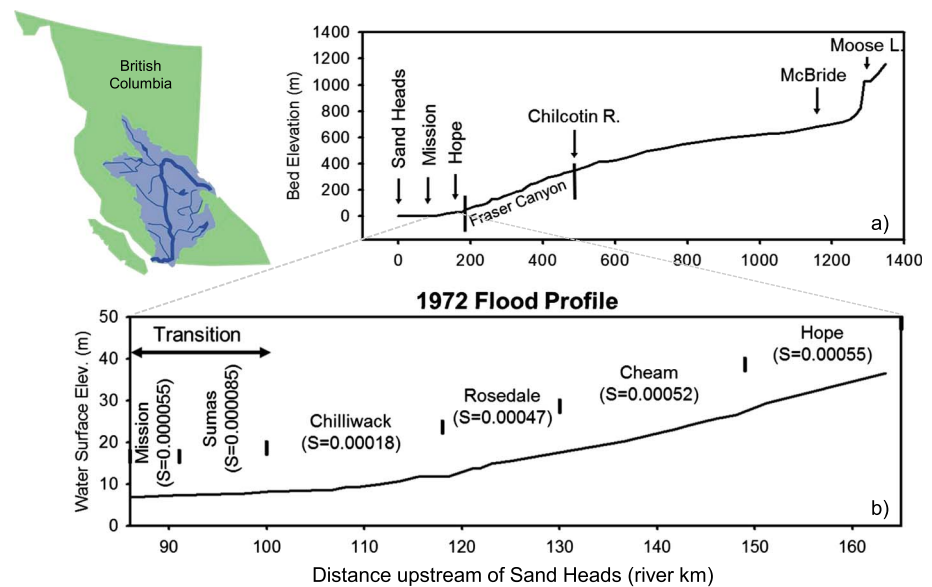


**Figure 1.** (a) Downstream change in river bed elevation in the Fraser River from the headwaters to the Strait of Georgia at Sand Heads. (b) The 1972 water surface profile during the annual freshet with the major reaches and their associated water surface slopes [from *McLean*, 1990]. The inset map shows the extent of the Fraser basin within British Columbia.

of the river in the Lower Mainland of BC. The lower alluvial reach of the river (Figure 2) begins at the exit of the canyons ~185 km from the sea, upstream of Hope, BC. The morphology of the river changes dramatically near Laidlaw at river kilometer (RK) 147 (upstream from Sand Heads, the mouth of the river). Between Laidlaw and Sumas Mountain (RK 90–100), immediately upstream from Mission (RK 85), the river exhibits a gravel-bedded wandering habit as it deposits its gravel load (Figure 2). Below Sumas Mountain, it adopts a sand-bedded, single-thread planform with bends, but most of the water is carried through the inside of the bends rather than the apices (Figure 2), so it is not actively meandering. At New Westminster (RK 34), the river enters its delta where it bifurcates and begins to deposit its sand load (Figure 2). Silt is deposited on the subaqueous distal margins of the delta in tidally dominated distributary channels and on tide flats that fringe the delta.

Flows in the river are dominated by the spring snowmelt in May–June. High flow occurs throughout late May, June, and early July and recedes in August and September. The mean annual flow at Mission, immediately downstream from the gravel-sand transition, is  $3410 \text{ m}^3 \text{ s}^{-1}$ ; the mean annual flood is  $9790 \text{ m}^3 \text{ s}^{-1}$  [*McLean et al.*, 1999], and the 1894 flood, in which flows are estimated to have reached  $17,000 \pm 1000 \text{ m}^3 \text{ s}^{-1}$  [*NHC*, 2008], is the historic flood of record. *McLean et al.* [1999], on the basis of analysis of river surveys and bed load transport measurements at Agassiz (RK 130.5) in the period 1966–1986, estimated the annual gravel influx into lower Fraser River to be about  $87,000 \text{ m}^3 \text{ a}^{-1}$  (mineral measure). A later compilation using surveyed bed level changes between 1952 and 1999 in the gravel-bedded reach [*Church et al.*, 2001] suggests that the figure may be closer to  $128,000 \text{ m}^3 \text{ a}^{-1}$  at Laidlaw, but this figure includes interstitial and cover sands. The true figure certainly is of order  $100,000 \text{ m}^3 \text{ a}^{-1}$ .

A 10 times reduction in flood water surface gradient is reported [*McLean et al.*, 1999] between Hope and Mission (Figure 1b). The river is tidally influenced at low flows to RK 100 where an increase in gradient prevents further penetration of tides. The reach within which the gravel-sand transition is thought to occur is shown in Figure 3. *McLean et al.* [1999] reported that sand is carried in suspension in the gravel-bedded part of the river at Agassiz and that the bed material and bed load are sand at Mission. Figure 3 shows three grain size distributions collected by *McLean* [1990] from bar surfaces that show that the river is composed of >70% unimodal gravel (median grain-size ( $D_{50}$ ) of 12 mm) on Yaalstrick Bar which terminates at RK 100.5. At Mission, the bed sediment is 0.34 mm sand with a small fraction of gravel. At Hatzic Bar the bed sediment, sampled from the bar head, is a bimodal gravel and sand mixture, which led *McLean et al.* [1999] to assert that the gravel-sand transition must lie somewhere between Yaalstrick Bar and Mission. Here we test this claim by detailed examination of grain size variability in the reach between Yaalstrick Bar and Mission and by looking at how river bed topography and channel hydraulics change through the alluvial Lower Fraser River.

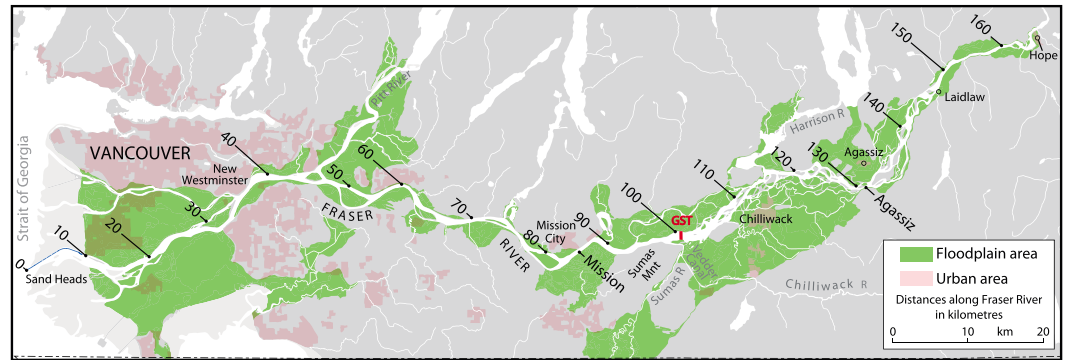


Figure 2. Lower Fraser River, British Columbia. GST marks the position of the gravel-sand transition.

3. Data

Our data set is composed of channel bed surveys from 1999 and 2008, water surface profiles collected in 1972, 1974, and 1999, and bed material sampling undertaken between 1983 and 2009. In this large river, net changes in the long profile and mean characteristics of bed material require centuries to achieve, so these data—gathered within a period of 37 years—can be regarded as contemporaneous. Detailed sampling in the reach of the river from immediately downstream of Yaalstrick Bar to Mission was undertaken in 2007 and 2008, and the data are consistent with those from the earlier surveys. The data from the 2007 and 2008 freshets correspond to a period of high flows in the river. During the 2007 freshet, flow at Hope peaked on 10 June at  $\sim 10,800 \text{ m}^3 \text{ s}^{-1}$  (return interval of 12 years), while at Mission flows peaked at  $\sim 11,900 \text{ m}^3 \text{ s}^{-1}$  (return interval of 8 years) (Figure 4). Flows at Mission remained above  $6000 \text{ m}^3 \text{ s}^{-1}$  through the end of July, after which flows declined into the low-flow season. The size of these flows ensures that the sediment transport processes responsible for the gravel-sand transition were active during the sampling period.

During the 2007 freshet, 33 bed material samples were recovered from the channel using a Shipek sampler at select locations. An additional 91 bed material samples were taken in the winter of 2008 at low flows with a dredge sampler (see Figure 4 for sampling periods). The low-flow sampling included samples taken at

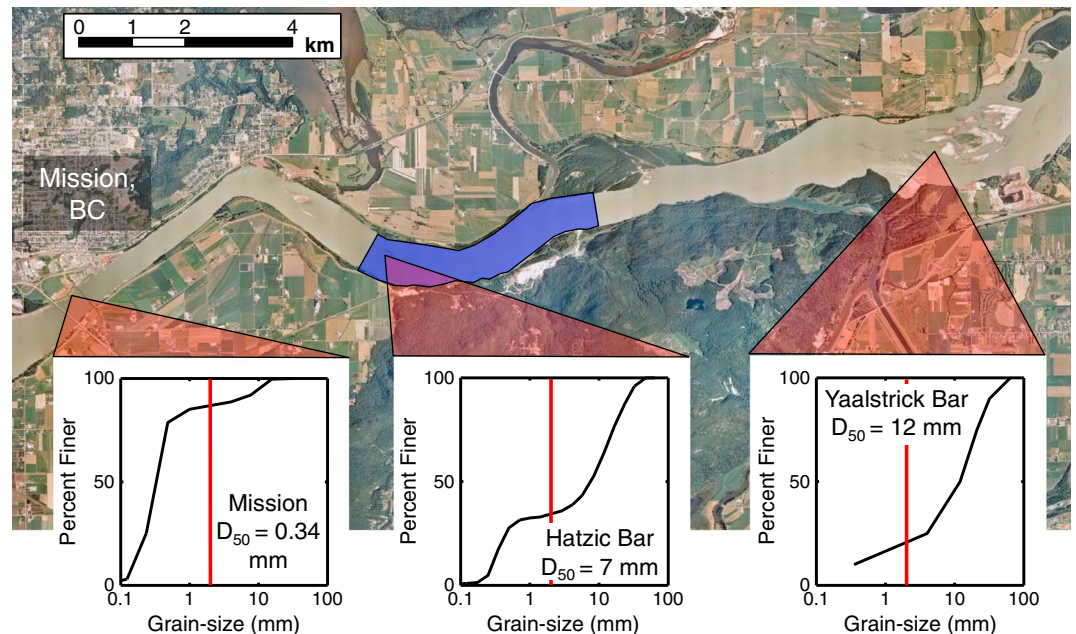
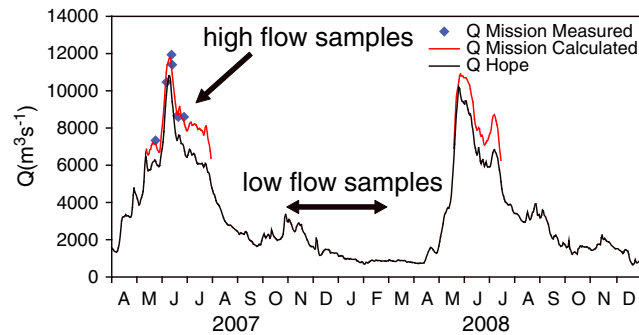


Figure 3. Reach of Fraser River where the gravel-sand transition has traditionally been thought to occur. Also indicated are three grain size samples reported by McLean [1990], the basis for placing the gravel-sand transition in the blue shaded area.





**Figure 4.** Hydrographs for Fraser River at Mission (Water Survey of Canada Station 08MH024) and Hope (WSC station 08MF005) for 2007 and 2008 with sampling periods shown. The WSC uses a rating curve to calculate discharge ( $Q$ ) at Mission only when the combined flow at Hope and the Harrison River, a tributary between Hope and Mission, exceeds  $5000 \text{ m}^3/\text{s}$  due to the tidal influence on water levels at lower flows. Bed sampling periods are shown.

samples should be considered as line samples with a length not exceeding a few meters. Both samplers combine surface and shallow subsurface material and recover of order 1 kg of material. On the sand bed, this weight is sufficient to meet the most stringent of sediment sampling standards proposed by Church *et al.* [1987], but in the instances when gravel was recovered, the more relaxed standards may or may not have been reached, depending on the size of the largest clasts. This constraint is inherent in the methods of recovery from deep water (10–30 m) available to us. Excessively small samples ( $<0.25 \text{ kg}$ ) or a few grains were discarded. As indicated below, the sampling method and constraints do not appear to have affected the recovered grain size distributions.

The high-flow samples were collected in sets of three across the channel and in locations where we suspected a gravel or sand cover based on concomitant multibeam echo sounding. At low flow, an attempt was made to collect samples systematically with two to three samples per cross section at 1 km intervals, but sampling sites were constrained by navigability. On Hatzic Bar (Figure 3), large samples were obtained when the bar was exposed. We separated the surface material from the subsurface material by removing exposed particles then digging into the bar to obtain a subsurface sample on Hatzic Bar. When all samples are considered, the sampling pattern is seemingly random. We explored displays of selected subsets of samples and found that the same textural patterns exist regardless of sampling pattern, the sampler used, or flow conditions.

To augment our data set, we incorporate bed material grain size information from a number of published sources including McLean [1990] (48 samples) and Ham [2005] (35 samples), who sampled bar surfaces between RK 85 and 160. These are subsurface samples of several hundred kilograms each, specifically calculated to meet the sampling standards of Church *et al.* [1987]. They were sieved in the field at  $0.5\phi$  intervals to 16 mm, and a subsample of finer materials returned to the laboratory for further separation. We also present data from McLaren and Ren [1995], who sampled bed material throughout the Fraser delta, including the main channel, distributary channels, and the delta front using a Shipek sampler. They obtained five samples per river cross section at 0.5 km increments along the channel from RK 48.5 into the Strait of Georgia. We present 480 of their samples from the main channel. At low flow in 2009, we added 33 bed material grain size samples between RK 85 and RK 48.5, collected every 5 km with the dredge sampler because no samples were available between RK 85 (our 2007/2008 data set) and RK 48.5 (the McLaren and Ren [1995] data). All of these samples consisting of sand and silt meet the most stringent sampling standards of Church *et al.* [1987].

We also present bathymetric data provided by Public Works and Government Services, Canada, collected during the 2008 freshet. Survey lines were spaced roughly 100 m apart, and elevations were obtained at submeter spacing along each line. These data were collected at high water, so they provide bank-to-bank spatial coverage. Data points have centimeter precision both vertically and laterally, but interpolation between sections may have larger vertical error. However, longitudinal consistency in mean bed elevation is high so that gross errors in mean channel topography are not expected. The data are not sufficiently detailed

approximately the same location as the high-flow samples. The Shipek and dredge samplers collect roughly the same volume of bed material, but the collection methods are different. The Shipek uses a weight and spring mechanism to scoop sediment at-a-point upon impact with the bed. The dredge sampler is dragged along the bed until it fills. The retrieved material may be from a point where the dredge excavated the bed surface, from a scrape along the drag line, or may consist of individual particles collected as the sampler skidded along the surface of the drag line. We discarded samples in which the sampler skidded along the bottom for a long distance. As such, the dredge

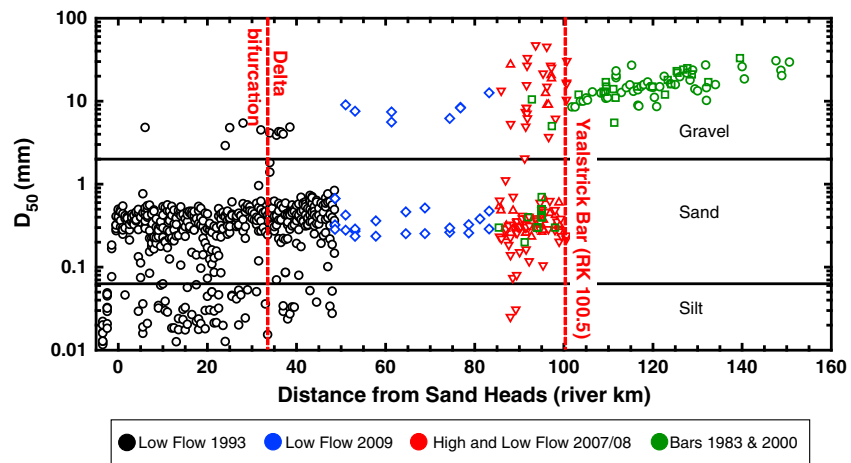


**Figure 5.** Downstream change in median bed material grain size ( $D_{50}$ ). Low-flow data from 1993 are from McLaren and Ren [1995], and gravel bar data from 1983 and 2000 are from McLean [1990] and Ham [2005], respectively. Upward and downward pointing red triangles are for high-flow (2007) and low-flow (2008) samples, respectively.

to observe bed forms in the channel that may have amplitudes of order 1 m and wavelengths  $<50$  m but do provide complete topographic information about channel-scale bed topography and bar morphology.

Our information about the along-stream channel hydraulics (flow depths and water surface slopes) also derive from a series of published sources. There has been no integrated, systematic study of flow in the lower Fraser River from Hope to Sand Heads, so the available information is piecemeal and spans many decades. We present a bed profile compiled by NHC [2006] from RK 0 (Sand Heads) to RK 85 (Mission) and Ham [2005] from RK 85 to RK 160. This bed profile was taken from a 1999 survey of the river by Public Works and Government Services, Canada, using the same methods as for the 2008 survey. The bed profile is calculated by averaging bed elevation across survey lines perpendicular to the flow (D. Ham, personal communication, 2009). Water Surface data for RK 0 to 90 are from NHC [2006] and based on gauge measurements. Water surface data for RK 85 to 160 are from 1972 and 1974 flood flows (reported in McLean [1990]). Ham [2005] reported a water surface profile for the 1999 flood flow: it is a smooth line, presumably a fit to gauge data, so water surface slopes calculated from this data should be viewed with caution. The recurrence intervals of the 1972, 1974, and 1999 flood flows are 50, 13, and 14 years, respectively. Some care needs to be taken with interpreting local values of the water surface slope, flow depth, and the boundary shear stress because of local changes in the river that occurred between the early 1970s, 1999, and the late 2000s. However, the broad patterns in slope, depth, and shear stress that are of interest here are likely to be consistent with present conditions.

## 4. Observations

### 4.1. Sediments Through the Lower Fraser River

Figure 5 shows the changes in median bed material grain size downstream of Hope. There is a clear downstream fining trend in the gravel that persists almost all the way to the ocean. Upstream of RK 100.5, all the samples are gravel sized. Most of the samples between RK 100.5 (the end of Yaalstrick Bar) and RK 0 (Sand Heads) are sand sized; 11.2% have a  $D_{50}$  that is silt sized and 8.2% are gravel sized. Between RK 100.5 and RK 48.5 (junction with the Pitt River and just upstream of where the channel begins to bifurcate as it enters the terminal delta), 23.4% of the samples have a  $D_{50}$  that is gravel sized. Beyond RK 48.5, the number of samples with  $D_{50} > 2$  mm is only 2.4%. Downstream of RK 100.5 there is no obvious downstream change in the size of the sand; however, once the river starts to bifurcate, there are more samples composed of silt-clay, obtained primarily along the channel margins. Grain size declines rapidly, moving seaward from Sand Heads into the Strait of Georgia (Figure 5).

There is a striking change in the bed material composition at RK 100.5. Figure 6 shows the cumulative fraction of gravel, sand, and silt downstream. Bed material goes from being composed of  $\sim 80\%$  gravel and  $\sim 20\%$  sand to being entirely sand over less than a kilometer at RK 100.5. Downstream of that point, the river bed sand

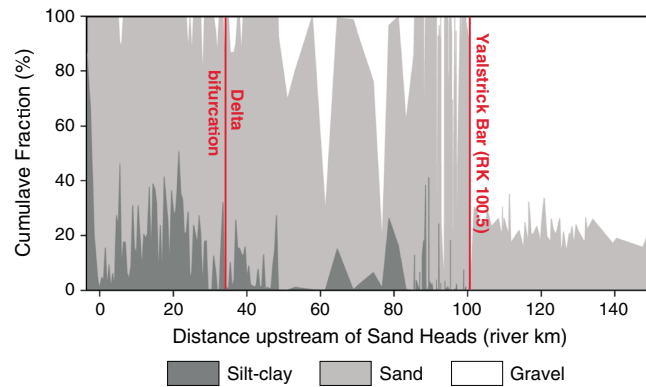


**Figure 6.** Fractional bed material size composition in Fraser River from Hope to Sand Heads. Data downstream of RK 85 were collected in cross sections, so each point is a cross-sectional average of two to four samples from RK 85 to 48.5 and five to eight samples from RK 48.5 to –3.5 (3.5 km offshore of Sand Heads). Data sources are given in Figure 5. The pattern of variation in the fine density reflects the variation in sample density.

transport. Nevertheless, some gravel is transported by the river bed well beyond the end of the gravel reach. The silt/clay content of the bed material is generally much greater downstream of RK 85, abruptly rising to >80% of the bed material as the river flows past the delta front at RK 0 and into the Strait of Georgia.

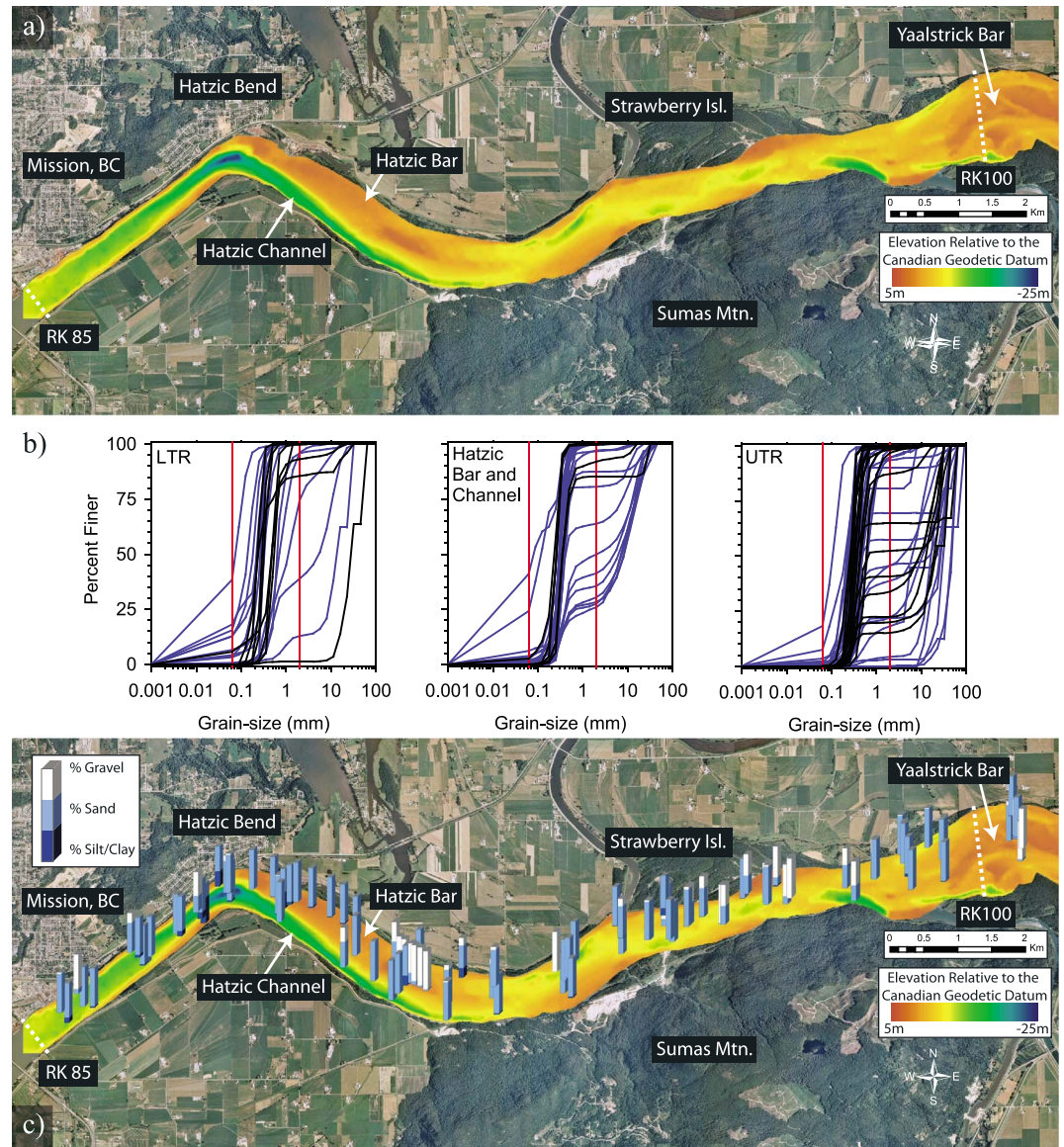
**4.2. Grain Size Variability in the “Transitional” Reach**

Figure 7a shows the bed topography through the transitional reach identified by *McLean* [1990], from immediately upstream of the end of Yaalstrick Bar to Mission. Several prominent topographic features are apparent. The subaqueous portion of Yaalstrick bar is composed of several streamlined lobes that taper downstream. There are multiple subchannels with a prominent channel on either side of the central bar, which is typical of medial bars in braided and wandering channels [*Rust*, 1978; *Church and Jones*, 1982]. The river is narrower and exhibits a sinuous thalweg downstream of Yaalstrick Bar between Sumas Mountain, where the river abuts bedrock, and Strawberry Island, which is part of the floodplain. Hatzic Bar is a large concave bank bench bar (in the sense of *Hickin* [1979]) formed by flow separation that occurs in the first major bend downstream of Yaalstrick Bar. The river is confined against the rip-rapped, but failing, southern bank adjacent Hatzic Bar, until the river exits Hatzic Bend, which is forced by high ground at Mission. Beyond this point the river is mainly unconfined (but today is diked). At Hatzic Bend, the bed is deeply scoured (Figure 7a). Moving downstream from Yaalstrick Bar to Mission, the river generally becomes deeper and narrower.

Figure 7b shows the grain size distributions of the bed material collected between Yaalstrick Bar and Mission in 2007 and 2008. There is no apparent difference between the patterns of gravel and sand revealed by the high- and low-flow grain size samples, so we combined the data sets. The majority of the samples are sand, but there are many bimodal distributions and a few samples that are pure gravel. The sand mode is centered at between 0.300 and 0.425 mm throughout the reach, a feature that persists all the way to the river mouth (Figure 5). Gravel samples from the thalweg are generally too small to accurately represent the grain size distributions according to the *Church et al.* [1987] criteria, so we focus on the percent gravel, sand, and silt/clay in each sample.

There are strong spatial patterns in bed material grain size through the reach (Figure 7c). Samples from the distal end of Yaalstrick Bar are gravel. The channel north of Yaalstrick Bar is a backwater channel and consequently is sand bedded (Figure 7c). The channel on the south side of the bar, which carries the majority of flow during freshet, is gravel bedded. Downstream of Yaalstrick Bar, the channel is almost entirely sand bedded with gravel appearing in some of the deeply scoured pools and on the bar heads that are immediately downstream of these pools. The prominent set of bar-head gravel samples on Hatzic Bar is the reason for the estimate of *McLean et al.* [1999] that the transition occurred in this vicinity. But the remainder of these bars is sand. This pattern is also well developed immediately upstream of Strawberry Island, where a scoured pool occurs on the southern side. The bed of the pool is a gravel-sand mixture that grades into a gravel bar head against the north bank.

content is near 100%, but there are some gravel patches downstream of RK 100.5. We suspect that they are limited in size based on the high-resolution sampling between RK 100.5 and 85. Our data between RK 85 and RK 48.5 are limited to 12 cross sections, two of which returned more than one sample of gravel-sized material, suggesting a significant gravel patch. Both are in channel constrictions, and one is adjacent to a ferry operation and may not be a natural deposit. Furthermore, gravel is barged downstream from a quarry at Sumas Mountain, and, in some winters, ice is rafted into the sand bed reach from upstream, so occurrences of gravel in this reach may indicate delivery mechanisms other than fluvial



**Figure 7.** (a) Bed topography through the gravel-sand transition reach of the Fraser river identified by *McLean et al.* [1999]. (b) Grain size distributions from the gravel-sand transition reach. UTR is the upper transitional reach (upstream of Hatzic Bar), and LTR is the lower transitional reach (downstream of Hatzic Bend). The red lines delimit sand size. Black and blue lines are the 2007 and 2008 samples, respectively. (c) Fractional bed material grain size. Each tricolor (dark blue, light blue, and white) bar represents one bed material sample. The proportion of a color on the bar indicates the percent of the sample composed of a particular size class. For example, the tricolor bar in the legend is 33.3% gravel, 33.3% sand, and 33.3% silt/clay.

The bars fine downstream and vertically downward. Figure 8 shows the bed surface texture on Hatzic Bar. The surface material on the bar head is unimodal gravel (Figures 8a and 8g location i) with a bimodal gravel-sand mixture immediately below the surface (Figure 8b) with ~30% sand (Figure 8g location i). Shallow trenches (~1 m deep) revealed that the material grades to sand with decreasing amounts of gravel (Figure 8c). Moving downstream along the bar, the coarse surface layer disappears and the surface is replaced with the bimodal gravel-sand mixture present in the subsurface upstream (Figures 8d and 8g location ii). Sand content (30–50%) is sufficient to indicate matric support of the deposit. Moving farther downstream along the bar, the gravel-sand mixture gives way abruptly to a sand surface and subsurface (Figures 8e and 8g location iii). The remainder of the bar is composed of sand with layers of silt-clay deposited from residual standing water in the troughs of low amplitude, symmetric, sand dunes, particularly toward the tail end of the bar (Figures 8f and 8g location iv).

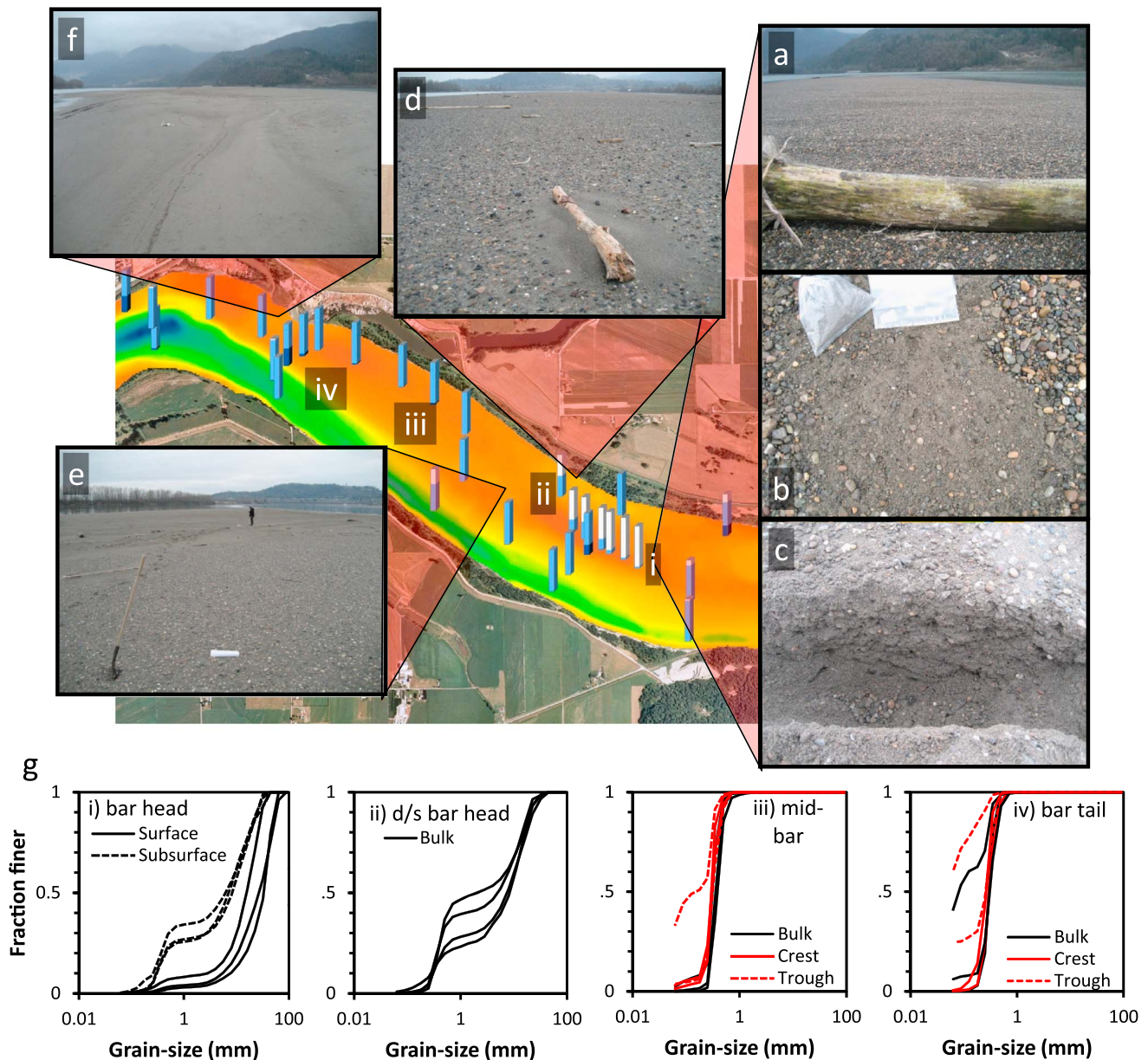


**Figure 8.** Sedimentology of Hatzic Bar. (a) Gravel surface veneer on head of bar, (b) sand-gravel mixture immediately below the gravel surface veneer, and (c) subsurface material in trench ~30 cm deep at location i (bar head). (d) Gravel-sand mixture downstream of the bar head at location ii (downstream of bar head). (e) View downstream of location ii looking toward location iii (midbar) showing the transition from a gravel-sand mix to a sand surface. (f) Sand surface with patches of finer silt-clay (in bed form troughs) on the bar tail at location iv. (g) Grain size distributions of samples collected along a northwest transect along Hatzic Bar. Bed topography and tricolor grain size bars are the same as in Figure 7c. Distributions labeled “crest” and “trough” refer to positions over low amplitude, symmetric, sand dunes developed on the bar with coarser crests and finer troughs. Distributions labeled “bulk” are where there was no obvious surface coarsening with respect to the subsurface.

Gravel is also found in the thalweg adjacent to Hatzic Bar and along the north bank downstream of Hatzic Bend. At least one sample from the deepest part of the bend (not shown here) is composed of a consolidated marine mud that underlies the Fraser River sediments, suggesting that at Hatzic Bend the river is scouring to the base of the modern fluvial sediments at high flows. It is not clear whether the gravel in the thalweg is a lag deposit or an active gravel bed.

#### 4.3. Downstream Change in Channel Hydraulics

Figure 9 shows the downstream changes in water surface elevation and bed elevation using the available data, and Table 1 summarizes the mean properties. At RK 90, there is a break in the bed slope. The bed

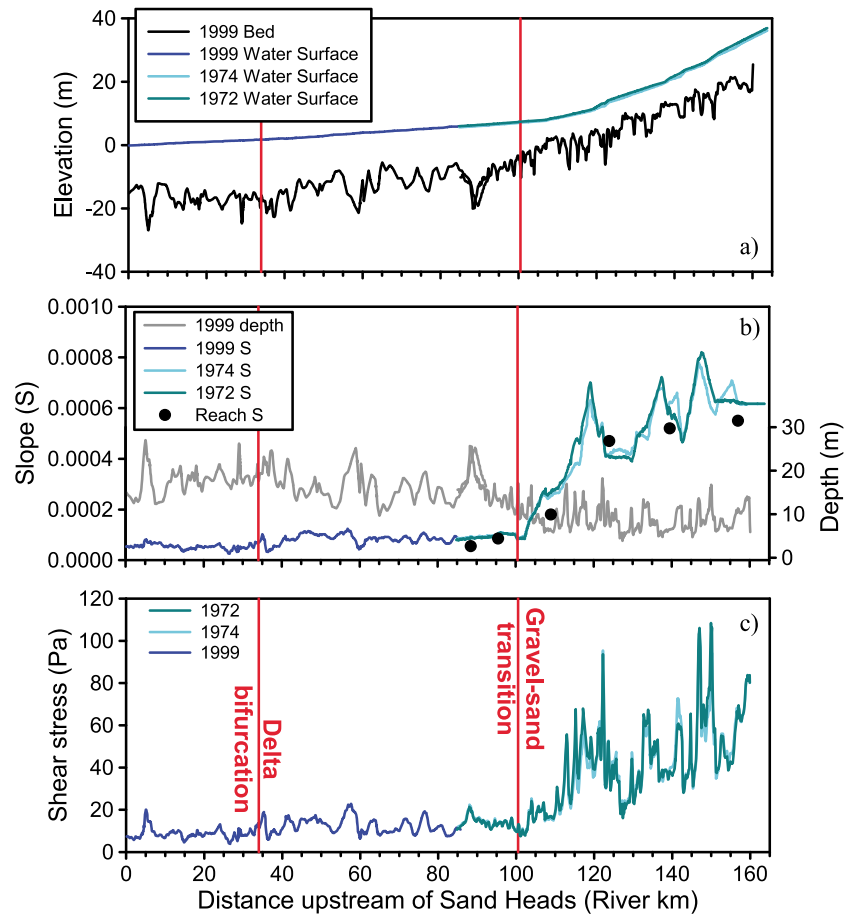


**Figure 9.** Downstream change in (a) bed and water surface elevation, (b) flow depth and water surface slope ( $S$ ), and (c) shear stress. Water surface elevations and slopes between RK 85 and 160 for 1999 are not displayed because they are a line fit rather than measured data. The mismatch between bed elevations centered at RK 90 is because we have combined data sets from different sources.

slope declines from  $4.286 \times 10^{-4}$  in the gravel-bedded reach to  $1.030 \times 10^{-4}$  in the sand-bedded reaches (Figure 9a). There is also a break in the flood water surface slopes in 1972 and 1974 that occurs upstream of the break in bed slope approximately at RK 102, beyond which the bed slope is nearly constant to the ocean (Figure 9b). This break is just upstream of the tail end of Yaalstick Bar, and we use it as the division between reaches for channel hydraulic calculations, even though the grain size change clearly occurs 1.5 km downstream. High-flow depth in the main channel of the gravel-bedded reach of the river, between RK 102 and 160, is ~10 m (Table 1 and Figure 9b). In the largely sand-bedded reach from RK 48.5 to RK 102, the flow depth is ~15 m. In the sand-bedded reach from RK 0 to 48.5, the flow depth was nearly double the depth in the gravel-bedded reach in 1999 at 18.6 m.

These patterns give rise to declining shear stress through the gravel-bedded reach of the river with a dramatic drop that begins at ~RK 110, reaching a value that is nearly constant to the ocean at RK 102 (Figure 9c). The total boundary shear stress is calculated from data in Figure 9b using the 1-D momentum balance for steady, uniform flow

$$\tau = \rho g S h \tag{1}$$

where  $\rho$  is the fluid density ( $1000 \text{ kg/m}^3$ ),  $g$  is gravitational acceleration,  $S$  is the water surface slope (calculated over a 5 km window), and  $h$  is the flow depth. In the gravel-bedded reach, the mean total shear stress is ~55 Pa during flood flows; through the largely sand-bedded reach from RK 48.5 to RK 102, the boundary shear stress is ~13 Pa, and from RK 48.5 downstream, the boundary shear stress is ~10 Pa (Table 1).

**Table 1.** Hydraulic Characteristics of the Gravel-Bedded Reach, the Dominantly Sand-Bedded Reach With the Diffuse Extension of the Gravel-Sand Transition (GST), and the Sand-Bedded Delta Reach of the Lower Fraser River

Reach	RK	$D_{50}$ (mm) Subsurface	Mean Bed Slope ( $10^{-4}$ ) <sup>d</sup>	Mean Width (m) <sup>e</sup>	Year	Mean Depth (m) <sup>f</sup>	Mean Water Surface Slope ( $10^{-4}$ )	Mean Shear Stress (Pa)
Gravel	102–160	16.1 <sup>a</sup>	4.286	876 (278–2037)	1972	10.2	4.71	52.8 <sup>h</sup>
					1974	10.7	4.83	56.8 <sup>h</sup>
					1999	9.2	4.07 <sup>i</sup>	38.9 <sup>h</sup>
Sand with diffuse GST extension	48.5–102	10/0.3 <sup>b</sup>	1.030	694 (375–1353)	1972 <sup>g</sup>	15.6	0.948	13.5
					1974 <sup>g</sup>	15.9	0.920	13.4
					1999	15.7	0.913	12.8
Sand	0–48.5	0.428 (0.383) <sup>c</sup>	1.030	792 (401–1245)	1999	18.6	0.608	10.3

<sup>a</sup>Mean of all samples upstream of RK 102 from *McLean* [1990].

<sup>b</sup>Approximate values based on the gravel and sand modes in Figure 7b.

<sup>c</sup>Mean of all samples between RK 0 and 48.5 from *McLaren and Ren* [1995]. The value in brackets is the mean of all sand-sized samples (gravel and silt-clay samples have been excluded).

<sup>d</sup>There is a distinct bed slope break at RK 90, and we calculate slope upstream and downstream of that slope break.

<sup>e</sup>Range in brackets.

<sup>f</sup>All calculated using bed topography for 1999 and water surface elevations for the respective year.

<sup>g</sup>There are no data for 1972 and 1974 from RK 0 to RK 85. Reported value is based on data from RK 85 to RK 102.

<sup>h</sup>Shear stresses are calculated for the gravel reach between RK 120 and 160 because at RK ~110 they begin to decline, and our goal in reporting the mean value is to give a representative value for this reach.

<sup>i</sup>The 1999 water surface profile between RK 85 and 160 is a smooth line fit to the water surface profile, so this value and the associated shear stress should be viewed with some caution.

## 5. Discussion

### 5.1. Where Is the Transition in Fraser River and What Is its Morphology?

Most research on gravel-sand transitions suggests that they are abrupt [cf. *Yatsu*, 1957; *Howard*, 1980; *Shaw and Kellerhals*, 1982; *Brierley and Hickin*, 1985; *Sambrook Smith and Ferguson*, 1995; *Dade and Friend*, 1998; *Cui and Parker*, 1998; *Parker and Cui*, 1998; *Knighton*, 1999; *Ferguson*, 2003; *Gran et al.*, 2006]. Some recent work [*Ferguson et al.*, 2011] has shown that downstream of an advancing gravel front with high sediment supply, a more diffuse transitional reach occurs, the transition appearing to be more patchy on the surface and more continuously gradational in the subsurface sediment, while *Singer* [2008, 2010] and *Frings* [2011] describe nonabrupt, extended transitions.

Previous work has placed the gravel-sand transition in the Fraser River just upstream of Hatzic Bar at RK 92 [*McLean*, 1990; *Ham*, 2005]. Our observations suggest that the transition is actually some distance upstream at the downstream end of Yaalstrick Bar, where it appears as a terminating gravel wedge. The spectacularly abrupt, visible terminus occurs at RK 100.5, based on the dramatic change in channel morphology (Figure 2), grain size (Figure 5), water surface slope, and shear stress that occurs there (Figure 9). The deposit also shifts from clast to matrix supported at RK 101.5 (Figure 6). Indeed, the downstream “front” of Yaalstrick Bar has the form of a miniature Gilbert delta, with the gravel face avalanching into the deeper water downstream. However, there are patches of gravel downstream of this gravel wedge, which suggests that there is a somewhat diffuse continuation of the sedimentological transition beyond the morphological wedge. Nevertheless, these patches appear merely as veneers on the bar surfaces or lag deposits in deeply scoured pools. These observations are circumstantially supported by observations of *Church and Rice* [2009], who measured bar heights through the gravel-bedded part of the river and found that bar amplitude more than doubles downstream of Yaalstrick Bar, suggesting a changed composition of the bars from gravel to sand, the latter being susceptible to carriage to greater heights above the river thalweg to be deposited on and build relatively higher bar surfaces.

### 5.2. How Does Gravel Mobility Change Across the Gravel-Sand Transition?

We explore this question by examining the mobility of various grain sizes using the nondimensional Shields stress calculated as

$$\tau_* = \frac{\alpha\tau}{(\rho_s - \rho)gD} \quad (2)$$

where  $\tau$  is from Figure 9c,  $\rho_s$  is the sediment mineral density ( $2650 \text{ kg/m}^3$ ),  $D$  is a grain size, and  $\alpha$  is the fraction of the total shear stress applied to the grains on the bed and therefore available to move sediment. We can estimate whether or not a particle is mobile by comparing the value of  $\tau_*$  to its critical value for entrainment,  $\tau_{*c}$ . If the ratio  $\tau_*/\tau_{*c} > 1$ , a particle is likely to be mobile. We can calculate the value of  $\tau_{*c}$  for a given particle size from the *Brownlie* [1981] fit to the Shields curve. There are some difficulties with this approach, namely, “hiding effects” that make small particles less mobile because they hide between larger particles that are less mobile. This effect makes unstructured gravel mixtures mobile at approximately a constant value of 0.045 [Miller et al., 1977; Yalin and Karahan, 1979]. There is also evidence that finer grains in sufficient quantity on the bed can make larger particles move more easily [Wilcock, 1998; Wilcock and Kenworthy, 2002; Venditti et al., 2010]. This reduces  $\tau_{*c}$  by about 2 times as sand coverage increases in the empirical model of Wilcock and Crowe [2003].

Finding an appropriate value of  $\alpha$  to calculate the effective shear stress is difficult. Stress calculated from the 1-D momentum balance (equation (1)) includes the stress applied to the granular bed and stress associated with form drag caused by macroscale features of the bed (bed forms, clusters, and stone cells), bars, banks, vegetation, and human-placed structures. These features cause a transfer of momentum from the mean flow to deviations from the mean flow (turbulent fluctuations and coherent flow structures), and channel morphology can cause secondary circulations which also draw momentum from the mean flow. It has often been supposed that form drag is minor in gravel bed rivers. For example, *Parker and Peterson* [1980] argued that form drag on bars in gravel-bedded rivers is negligible; however, others have argued that it can be significant [cf. *Millar*, 1999], and there is evidence that the structure of a gravel bed can significantly increase  $\tau_{*c}$  [Church et al., 1998]. There is no generally accepted method to determine the effective shear stress for channels with complex morphology. Simple form drag corrections [e.g., *Wiberg and Smith*, 1987; *Lamb et al.*, 2008] do not incorporate all the possible sources of form drag or momentum transfers to secondary circulations, so a more heuristic approach to finding the value of  $\alpha$  is necessary.

Here we use two different methods to estimate the value of  $\alpha$  in the gravel reach of Fraser River. The first method takes advantage of the fact that in gravel-bedded rivers, the bed surface is typically coarser than the subsurface grain size distribution, which is often considered to be equivalent to the bed load grain size. This occurs because the subsurface was deposited from the bed load while the surface has been modified by subsequent selective entrainment of finer materials or by their settlement through openings between the larger surface clasts. Fraser River gravels generally exhibit a coarse surface layer, often equivalent to the subsurface sediment truncated at about 8 mm [Church et al., 1987; McLean, 1990] but sometimes exhibiting a concentration of coarser sediment. It is reasonable to suppose that this layer controls initial gravel entrainment but that the subsurface material more fairly represents the size distribution of the bed load [see *McLean et al.*, 1999, Figure 8]. But the latter can be entrained only when the surface material has been mobilized. Equation (2) is inversely linear in  $\tau_*$  and  $D$ . If we accept the notion that the threshold for mobility of the  $D_{50}$  size in a mixture represents the threshold for the mixture, the value of  $\alpha$  can be calculated on the basis that the actual stress must be sufficient to mobilize the surface in order for the subsurface to be free to move. The critical Shields number to move the bed is

$$\tau_{*c} = \tau / (\gamma D_{50\text{surf}}) = \alpha \tau / (\gamma D_{50\text{sub}}) \quad (3)$$

where  $D_{50\text{surf}}$  and  $D_{50\text{sub}}$  are the median sizes of the surface and subsurface material and  $\gamma = g(\rho_s - \rho)$ . Therefore,  $\alpha = D_{50\text{sub}}/D_{50\text{surf}} = \tau_{*c\text{surf}}/\tau_{*c\text{sub}}$  where  $\tau_{*c\text{surf}}$  is the critical Shields number for the bed surface material and  $\tau_{*c\text{sub}}$  is the Shields number at the same shear stress for the bed subsurface material.

We can estimate values of  $\alpha$  from previous work in the gravel-bedded reach of the river. For example, *McLean et al.* [1999], on the basis of a program of bed load measurements using basket traps, estimated that gravel begins to move in the gravel-bedded reach at Agassiz (RK 130.5) at  $Q = 5000 \text{ m}^3 \text{ s}^{-1}$ . At this flow,  $h = 5.2 \text{ m}$ . Water surface slope at Agassiz is  $4.8 \times 10^{-4}$ ,  $D_{50\text{surf}} = 42 \text{ mm}$ , and  $D_{50\text{sub}} = 25 \text{ mm}$  [McLean et al., 1999]. On these data,  $\tau_{*c}$  for surface sediment is 0.036, while  $\tau_*$  for the subsurface  $D_{50}$  at this flow is 0.061, the difference arising from the difference in grain size. Hence, for local gravel entrainment at Agassiz,  $\alpha = 0.60$ . Downstream of Agassiz, from RK 110 to 116, *Rennie and Church* [2010] obtained detailed measurements of flow depth, velocity, and shear velocity ( $u_*$ ) at a discharge of  $6000 \text{ m}^3 \text{ s}^{-1}$ . They showed that the reach was very near threshold for local bed mobilization using an acoustic Doppler current profiler. The observed mean value of  $u_*$  was  $0.14 \text{ m s}^{-1}$  [Rennie and Church, 2010, Table 1]. The local bed material sizes are  $D_{50\text{surf}} = 27 \text{ mm}$  and  $D_{50\text{sub}} = 13.3 \text{ mm}$  in



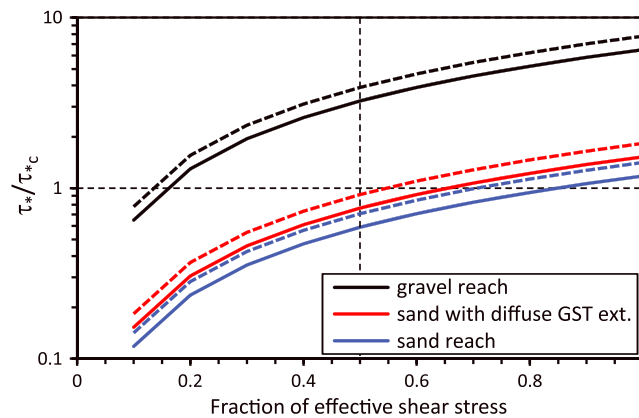


**Figure 10.** Mobility of 12 mm (solid lines) and 10 mm (dashed lines) gravel mixtures as a function of effective shear stress (fraction of total) in the gravel-bedded portion of the river (RK 120–160), the largely sand-bedded diffuse gravel-sand transition extension (RK 48.5–102), and the sand-bedded reach (RK 0–48.5). Calculations based on 1974 flood flow water surface profile and 1999 bed profile between RK 85 and 100 and the 1999 bed and water surface profile from RK 0 to 85.

this area [Church and Ham, 2004], leading to  $\tau_{*c\text{surf}} = 0.045$  for the surface  $D_{50}$  and  $\tau_{*c\text{sub}} = 0.091$  for the subsurface  $D_{50}$ . For the local bed, we have  $\alpha = 0.50$ . At Yaalstrick Bar where we know the gravel mixture stops moving,  $D_{50\text{surf}} = 20$  mm while  $D_{50\text{sub}}$  is 12 mm so that  $\alpha = 0.6$ . If we follow the fining trend in Figure 5,  $D_{50\text{sub}}$  should be closer to 10 mm at RK 100.5 so that  $\alpha = 0.5$ .

Another method to estimate  $\alpha$  is to take advantage of the fact that we know where general motion of the gravel mixture ceases in the system. We can then use an inverse method to calculate the value of  $\alpha$  where we know  $\tau^*/\tau_{*c} \approx 1$ . Figure 10 shows  $\tau^*/\tau_{*c}$  for a range of different values of  $\alpha$  for the gravel bedded, the largely sand-

bedded diffuse gravel-sand transition extension, and the sand-bedded reaches. Using  $D_{50\text{sub}}$  at Yaalstrick Bar (10 and 12 mm),  $\tau^*$  is calculated for flood flows. We assume  $\tau_{*c} = 0.045$ . Figure 10 demonstrates that in the largely sand-bedded diffuse gravel-sand transition extension, where we know the gravel is only marginally mobile ( $\tau^*/\tau_{*c} \approx 1$ ), the fraction of total shear stress at which the subsurface gravel mixture stops moving is 0.5 for 10 mm gravel and 0.6 for 12 mm gravel. In the gravel-bedded reach of the river, gravel is mobile as long as  $\alpha > 0.2$  and it is not mobile in the sand-bedded reach unless  $\alpha > 0.7$ , which is certainly not the case because there are bed forms in the sand-bedded reach.

Both methods and the associated data lead to the conclusion that  $\alpha$  is approximately 0.5 to 0.6. Figure 11 shows how  $\tau^*$  changes relative to  $\tau_{*c}$ , calculated from the fit to the Shields curve [Brownlie, 1981] using  $\alpha = 0.5$  for flood flow water levels. The selection of a constant or variable value of  $\tau_{*c}$  affects the magnitude of  $\tau^*/\tau_{*c}$  but not the patterns in Figure 11. Regardless of grain size,  $\tau^*/\tau_{*c}$  declines through the gravel-bedded reach of the river to RK 102, beyond which there is a more gentle decline to the ocean (Figure 11). The pattern suggests that the gravel-sand transition emerges because the gravel fractions cease moving.

The foregoing argument explains why the gravel wedge terminates abruptly at RK 100.5, but it does not explain the appearance of the gravel patches we observe downstream of Yaalstrick Bar. We strongly suspect that the deposits formed on the bar heads are caused by the superior mobility of gravel over sand. It is well recognized that the addition of sand to a gravel mixture will increase gravel transport rates in river channels [Jackson and Beschta, 1984; Iseya and Ikeda, 1987; Wilcock and McArdeall, 1993, 1997; Wilcock, 1998; Wilcock et al., 2001; Wilcock and Kenworthy, 2002; Curran and Wilcock, 2005]. Venditti et al. [2010] demonstrated that the phenomenon is produced by a hydraulic smoothing effect on the bed. They showed that the addition of sediment  $\sim 1/4$  the size of the bed surface material increases near-bed velocity and reduces turbulence, resulting in fluid acceleration in the near-bed region. This disproportionately increases drag exerted on the coarsest particles in a sediment mixture because the largest particles protrude farthest into the flow, promoting their mobilization.

We hypothesize that gravel may still be carried as bed load on top of the sand due to this hydraulic smoothing effect, even when the mobility of the gravel mixture is below the normal threshold for motion of  $\tau^* = 0.045$  [cf. Wilcock and Crowe, 2003; Venditti et al., 2010]. The gravel continues to move over the sand bed due to a lack of distrainment sites when fine sediment has covered the pockets between larger particles—the places where large particles often stop moving. We suspect a small gravel load rides over the sand beyond the gravel front. This gravel is gravitationally sorted into the pools where it may stop because, there, like-sized particles provide distrainment sites (cf. the “patch” effect of Paola and Seal [1995]). Accordingly, we suggest that the gravel deposits downstream of the gravel front are formed by gravel “leaking” out of the gravel-bedded part of the river and preferentially moving into the deep scour holes and onto bar heads.

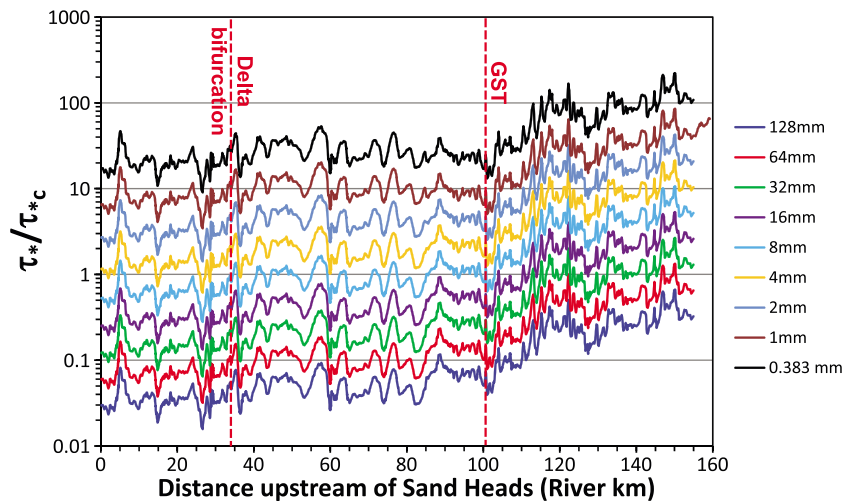


**Figure 11.** Downstream change in fractional mobility of sediment in the Fraser River using an effective shear stress ( $\alpha$ ) of 0.5. Data based on 1974 flood flow water surface profile and 1999 bed profile between RK 85 and 100 and the 1999 bed and water surface profiles from RK 0 to 85.

### 5.3. What Controls the Location of the Gravel-Sand Transition?

The reason gravel-sand transitions emerge at a particular location has been attributed to external controls on river gradient as well as autogenic processes such as the breakdown of specific lithologies of sediment directly from pebbles to sand, producing a grain size gap [Yatsu, 1957; Shaw and Kellerhals, 1982; Wolcott, 1988]. More recent work has shown that the latter, unusual, circumstance is not necessary to produce the bimodal sediment required for a gravel-sand transition and that the emergence of transitions can be controlled autogenically by sorting processes [e.g., Ferguson, 2003].

There is no evidence that the location or morphology of the Fraser gravel-sand transition is linked to the abrasion of particles in the gravel-bedded portion of the river. The gravel mode of the grain size distributions at the gravel front has a size  $\sim 10$  mm, which is the size that is usually described as being unstable and breaking down to sand-sized particles in some lithologies. But in Fraser River, the lithologies are mostly resistant igneous and metamorphic types that have survived glacial cycles. The 0.3–0.4 mm sand downstream of the gravel front is present in slack-water deposits throughout the Fraser Canyon as well, suggesting that its source may be several hundreds of kilometers upstream of the gravel-bedded reach of the lower river.

There are two interconnected external controls on the current position of the gravel-sand transition. The position coincides with a dramatic change in slope that occurs at Sumas Mountain and with the upstream limit of the backwater effect caused by the ocean tides. It is difficult to know whether the emergence of the gravel wedge is the cause or the effect of the break in slope. But there is evidence that sorting processes play an important role in the location of the transition because of the bimodal sediments that dominate the reach downstream of the gravel wedge and the decline in the shear stress associated with the change in gradient.

Ferguson and collaborators (see references throughout) argue that abrupt gravel transitions occur because the relation between shear stress and sediment transport is nonlinear. Ferguson *et al.* [1998], in particular, argue that as shear stress declines, coarser particles are deposited and finer particles are selectively transported. The bed becomes finer moving downstream as the coarser particles are removed from the upstream sediment supply. Ferguson [2003], building on a suggestion by Wilcock [1998], further argues that the abruptness arises because sand coverage is increasing. As sand makes up a greater portion of the bed surface, transport rates of both sand, and to a lesser extent gravel, increase. This increases the downstream sand supply relative to gravel. The shift occurs where a critical sand coverage on the gravel bed, in the range 20–30%, occurs. So where there is a strong downstream gradient in the sand coverage, the transition will be abrupt. In Fraser River, the sand fraction in bed sediments increases steadily through the gravel reach from a low of about 17% in proximal samples to a median value of 25% at Yalstrick Bar, with a maximum in individual samples of about 30% [Church and Ham, 2004]. The latter figures mark the onset of matric support for the gravel sizes and potentially substantially increased mobility.

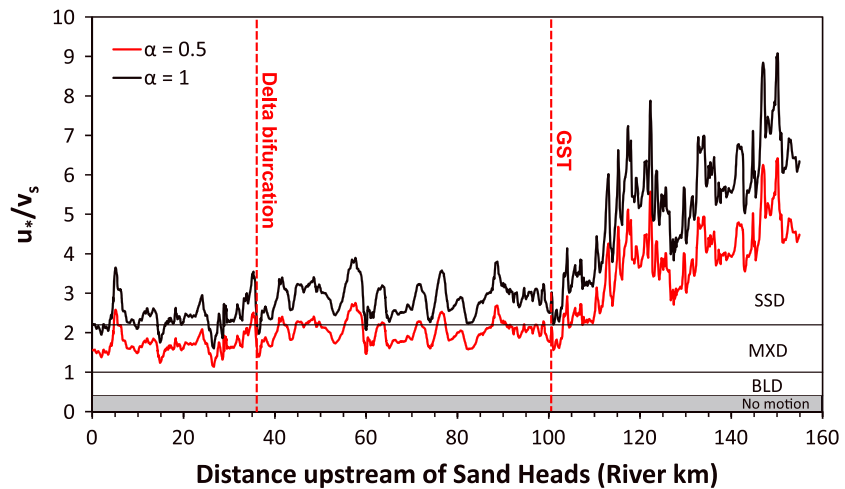


**Figure 12.** Downstream change in mobility of 0.383 mm sand in the Fraser River using an effective shear stress ( $\alpha$ ) equal to 0.5 and 1. Data based on 1974 flood flow water surface profile and 1999 bed profile between RK 85 and 100 and the 1999 bed and water surface profiles from RK 0 to 85. The horizontal lines show transport stages SSD (suspended load-dominated), MXD (mixed load-dominated), BLD (bed load-dominated), and no motion for 0.383 mm sand, calculated using the criterion in Church [2006], adjusted so the division between MXD and BLD occurs at  $u_*/v_s = 1$ .

There is direct evidence that a change in the dominant mode of sand transport occurs at RK 102. We can judge the mode of transport of the 0.3–0.4 mm sand by comparing the shear velocity  $u_*$  against the settling velocity of the sand  $v_s$ . Sediment is moved as bed load when  $\tau_*/\tau_{*c} > 1$  and can be suspended when  $u_*/v_s > 1$  [Bagnold, 1966; Nino and Garcia, 1998; Lopez and Garcia, 2001]. Suspension becomes the dominant mode of transport when  $\tau_*/\tau_{*c} > 33$  [Church, 2006] which corresponds to  $u_*/v_s > 2.2$  for 0.383 mm sand ( $v_s$  is calculated from the relation of Dietrich [1982]). Combining the thresholds for bed load and suspension, this suggests that a mixed load condition occurs when  $1 < u_*/v_s < 2.2$  and bed load conditions dominate when  $u_*/v_s < 1$ .

Figure 12 shows the ratio  $u_*/v_s$  with  $u_*$  calculated as  $\sqrt{\alpha\tau/\rho}$  for the flood flow conditions shown in Figure 9c. The condition  $\tau_*/\tau_{*c} > 1$  is true in all reaches of the river (Figure 11), so sand can be carried as bed load. Figure 12 shows that there is a striking decline in  $u_*/v_s$  through the gravel-bedded reach of the river and a more subtle decline approaching the ocean. For  $\alpha = 1$ , Figure 12 shows that  $u_*/v_s > 4$  in the gravel-bedded reach of the river, and between 2 and 4 downstream. But adopting our more reasonable value for the effective shear stress fraction of 0.5, the mean  $u_*/v_s$  is 3.9 for the gravel-bedded reach and 1.9 in the downstream reaches. This suggests a shift from a suspension-dominated condition to a mixed-dominated condition at RK 102, so more sand settles onto the bed. Therefore, sand is being delivered to the bed, increasing the sand coverage, overwhelming the gravel load and causing a shift to a sand-bedded river.

#### 5.4. Comparison to Other Systems

In Fraser River the gravel-sand transition is represented by an abrupt termination of the gravel reach at RK 100.5, signaled by an important hydraulic change at RK 102. It is followed by an ~50 km “diffuse extension” in the dominantly sand reach, the consequence of enhanced mobility of fine gravel over the sand bed. There are a number of other gravel-sand transitions in large rivers that present useful contrasts and similarities to what we see in the Fraser River.

An instructive contrast is the gravel-sand transition in the Rhine River [Frings, 2011]. At about  $9000 \text{ m}^3 \text{ s}^{-1}$ , the mean annual flood is roughly equivalent to that in Fraser River. The river gradient change through the Rhine transition, from  $2.0 \times 10^{-4}$  to  $1.1 \times 10^{-4}$ , is similar to the Fraser:  $1.8 \times 10^{-4}$  immediately upstream of the transition (Figure 1) to  $1.030 \times 10^{-4}$  in the sand reach (Table 1). Mean river width in the Rhine is 250 to 440 m, significantly less than Fraser River (700 to 850 m and highly variable, Table 1). The Rhine is a single-thread channel throughout and is fixed in a series of meander bends: the course of the river has been constrained by human action for many centuries. The Fraser, in contrast, is a wandering channel through the gravel reach and is essentially straight in the approach to the main transition and immediately downstream. The result is a gravel-

sand transition in the Rhine that occurs over 50 km with a diffuse extension for a further 70 km [see *Frings*, 2011, Figures 2 and 6]. The reason for the extended transition is flow through the meander bends, the hydraulics of which preserves patches of gravel in the outer (concave bank) part of each bend while promoting sand deposition in the inner side of the bend. Once established, sediment patch dynamics reinforce the sedimentological pattern [*Nelson et al.*, 2010]. Shear stress calculations confirm hydraulic control of the bends in establishing this pattern. The gradient decline is, accordingly, continuous rather than abrupt [*Frings*, 2011, Figure 1], further suggesting that the sedimentation feeds back into a gradient control. Interestingly, the diffuse extension in the Rhine is ascribed to lateral variations in the channel hydraulics. The location of gravel deposits, particularly the bar-head deposits, in Fraser River can be viewed similarly, whence we observe that lateral variations in hydraulics and sediment sorting, strongly present only in large rivers, are a major determinant of the sedimentology downstream from the primary gravel to sand transition.

The extended transition presented by *Singer* [2008, 2010] has quite different antecedents. He argues that a major reduction in sediment supply, including a virtual cessation of gravel recruitment through the twentieth century, has led to the patchy deposition of sand in the main thalweg of the river, while gravel size has declined in comparison with relict deposits on high bar surfaces. A further perturbing factor is regulation of flows, though in most reaches maximum flows are not much reduced. Hence, he describes a “gravel-sand transition” that extends over 175 km along the river, and he predicts an eventual regression of the transition to the upstream head of this reach. We disagree with this interpretation on the basis of our definition of a gravel-sand transition. What *Singer* [2008, 2010] describes is a temporal transition in sediment transport dynamics that may take centuries to complete and cannot be construed as a normal autogenic gravel-sand transition. It is a temporary change in grain size caused by a secular change in sediment supply and flow regulation which has led to deposition of sand in the channel. Indeed, examining the distribution of sand and gravel deposits in the system [*Singer*, 2008, Figure 2], it is clear that the historic gravel-sand transition in the Sacramento River was entirely similar to that in the Fraser River, with an abrupt transition at RK 225 above the mouth, the sedimentology of which is still evident today. Sand deposits similar to those described by *Singer* [2008, 2010] do occur in the Fraser River, but in this largely undisturbed river they appear as cover sands on bar tops and channel fills in seasonal secondary channels in the gravel bed reach, not in the main channel, and they are strongly transient.

In the case studied by *Ferguson et al.* [2011] in the Vedder “canal” (a tributary of the Fraser near RK 98; Figure 2)—in some respects an approximately one-tenth scale model of Fraser River—the progradation of gravel is occurring into a sand bed reach established in 1928 as the result of river rectification. There was initially no slope change in the reach, the design gradient being  $2.8 \times 10^{-4}$ . In the decades since, the proximal reach, where gravel has been deposited, has increased gradient to  $8 \times 10^{-4}$  while the distal gradient, largely through sand deposition, has increased to  $6 \times 10^{-4}$ . The differential change is slight but gives an indication of a developing slope break within the reach between the portion that is gravel-dominated and that which remains sand dominated. The gradient on the distal portion of the upstream gravel reach (that is, immediately above the rectified reach) is  $2 \times 10^{-3}$ , suggesting that a substantial further gradient increase in the gravel-dominated portion of the canal may be anticipated.

There is no general agreement about why gravel-sand transitions emerge, but they are commonly associated with a break in slope [*Sambrook Smith and Ferguson*, 1995] that causes a rapid decline in the boundary shear stress in the channel and decreases the mobility of coarser bed material and suspension of the coarser part of the sand load. In the Fraser River the abrupt decline in water surface slope near RK 102 dominates the change in hydraulic conditions, in particular the change in shear stress that drives the discrimination between gravel-dominated and sand-dominated bed conditions. The final question remains, then, how does such an abrupt change develop? A decline in competence is associated with any river as gradient declines on the final approach to base level. That decline may initially be smooth, but if the river upstream is competent to move gravel, it must at some point cease to have that ability. Once the limit of gravel has been established, the gradient above the transition will increase as gravel continues to accumulate and the deposit may prograde downstream, while below the transition, gradient may not increase: this action reinforces the change in shear stress at the point of transition. The gradient contrast across a developed gravel-sand transition may, fairly straightforwardly then, be a consequence of the sedimentological history associated with the inception and development of the transition.

## 6. Conclusions

Examination of the downstream change in bed material in the Lower Fraser River indicates that an abrupt gravel-sand transition emerges at the tail end of Yaalstrick Bar at RK 100.5 in the form of a terminating gravel wedge in the Fraser River. Patches of gravel downstream of the wedge form a diffuse extension. The location of the transition coincides with a dramatic decrease in the boundary shear stress. We propose that the break in water surface slope that causes this change in shear stress is a consequential feature of the transition. We show that the location of the transition occurs because of a decline in the mobility of gravel and deposition of sand from suspension that overwhelms the gravel bed, forcing a transition to a sand bed. We argue that the patches of gravel observed beyond the wedge are caused by enhanced mobility of gravel in the presence of sand. Our primary transition occurs, then, over a distance of barely more than a kilometer, with a diffuse extension that extends to the delta bifurcation.

This transition is similar in morphology and sedimentology to most others that have been defined in the literature and can be considered as an archetypical example, but counterexamples have been documented where river morphology strongly conditions patterns of sediment deposition or where secular change in sediment supply or streamflow have created transient conditions of sedimentation. Our results warrant direct observations of shear stress, gravel mobility, and suspended sediment flux downstream of the transition to test the hypotheses we have put forward concerning the factors that control localization of the gravel-sand transition.

## Acknowledgments

This work was supported by the Natural Sciences and Engineering Research Council of Canada (NSERC) Discovery grants to J.G.V. and M.C. The high-flow bed material samples were collected in collaboration with Mead Allison (Tulane University) and Jeffery Nittrouer (Rice University). Technical support and field assistance were kindly provided by Robert Humpheries (SFU), Brooke Webber (SFU), Laurel Eyton (SFU), Dan Haught (SFU), and Dan Duncan (Tulane University). We appreciate helpful reviews from R. Frings, M.B. Singer, and one anonymous referee and insights from the journal's Associate Editor. All data presented in this paper are freely available from the corresponding author (J.V.).

## References

- Bagnold, R. A. (1966), *An Approach to the Sediment Transport Problem for General Physics*, U.S. Geol. Surv. Prof. Pap. 422-I, Geological Survey, Washington, D. C.
- Brierley, G. J., and E. J. Hickin (1985), Downstream gradation of particle sizes in the Squamish River, British Columbia, *Earth Surf. Processes Landforms*, *10*, 597–606.
- Brownlie, W. R. (1981), Prediction of flow depth and sediment discharge in open channels, *Report No. KH-R-43A*, W. M. Keck Laboratory of Hydraulics and Water Resources, California Institute of Technology, Pasadena, Calif., 232 pp.
- Church, M. (2006), Bed material transport and the morphology of alluvial river channels, *Annu. Rev. Earth Planet. Sci.*, *34*, 325–354, doi:10.1146/annurev.earth.33.092203.122721.
- Church, M., and D. Ham (2004), Atlas of the alluvial gravel-bed reach of Fraser River in the Lower Mainland, Dep. Geography, The Univ. of British Columbia. Fraser River Project Report: ii+55 pp. [Available at [www.geog.ubc.ca/fraserriver/reports/](http://www.geog.ubc.ca/fraserriver/reports/)]
- Church, M., and D. Jones (1982), Channel bars in gravel-bed rivers, in *Gravel-Bed Rivers: Fluvial Processes, Engineering and Management*, edited by R. D. Hey, J. C. Bathurst, and C. R. Thorne, pp. 291–324, John Wiley, Chichester.
- Church, M., and R. Kellerhals (1978), On the statistics of grain size variation along a gravel river, *Can. J. Earth Sci.*, *15*, 1151–1160.
- Church, M., and S. P. Rice (2009), Form and growth of bars in a wandering gravel-bed river, *Earth Surf. Processes Landforms*, *34*, 1422–1432, doi:10.1002/esp.1831.
- Church, M., D. G. McLean, and J. F. Wolcott (1987), River-bed gravels: Sampling and analysis, in *Sediment Transport in Gravel-Bed Rivers: Proceedings of the 2nd International Gravel-Bed Rivers Workshop*, edited by C. R. Thorne, J. C. Bathurst, and R. D. Hey, pp. 43–87, John Wiley, Chichester.
- Church, M., M. A. Hassan, and J. F. Wolcott (1998), Stabilizing self-organized structures in gravel-bed stream channels, *Water Resour. Res.*, *34*, 3169–3179, doi:10.1029/98WR00484.
- Church, M., D. G. Ham, and H. Weatherly (2001), Gravel management in Lower Fraser River, Report for the City of Chilliwack, xi+110 pp. [Available at [www.geog.ubc.ca/fraserriver/reports/](http://www.geog.ubc.ca/fraserriver/reports/)]
- Cui, Y., and G. Parker (1998), The arrested gravel front: Stable gravel-sand transitions in rivers Part II—General numerical solution, *J. Hydraul. Res.*, *36*, 159–182.
- Curran, J. C., and P. R. Wilcock (2005), The effect of sand supply on transport rates in a gravel-bed channel, *J. Hydraul. Eng.*, *131*, 961–967, doi:10.1061/(ASCE)07339429(2005)131:11(961).
- Dade, W. B., and P. F. Friend (1998), Grain-size, sediment transport regime, and channel slope in alluvial rivers, *J. Geol.*, *106*, 661–675.
- Dietrich, W. E. (1982), Settling velocity of natural particles, *Water Resour. Res.*, *18*, 1615–1626, doi:10.1029/WR018i006p01615.
- Ferguson, R. I. (2003), Emergence of abrupt gravel to sand transitions along rivers through sorting process, *Geology*, *31*, 159–162.
- Ferguson, R. I., T. B. Hoey, S. J. Wathen, A. Werritty, R. I. Hardwick, and G. H. Sambrook Smith (1998), Downstream fining of river gravels: An integrated field lab and modeling study, in *Gravel-Bed Rivers in the Environment: Proceedings of the 4th International Workshop on Gravel-Bed Rivers*, edited by P. Klingeman et al., pp. 85–114, Water Resource Publications, Lakewood, Colo.
- Ferguson, R. I., D. J. Bloomer, and M. Church (2011), Evolution of an advancing gravel front: Observations from Vedder Canal, British Columbia, *Earth Surf. Processes Landforms*, *36*, 1172–1182.
- Ferguson, R., T. Hoey, S. Wathen, and A. Werritty (1996), Field evidence for rapid downstream fining of river gravels through selective transport, *Geology*, *24*, 179–182.
- Frings, R. M. (2011), Sedimentary characteristics of the gravel-sand transition in the River Rhine, *J. Sediment. Res.*, *81*, 52–63, doi:10.2110/jsr.2011.2.
- Gran, K. B. (2012), Strong seasonality in sand loading and resulting feedbacks on sediment transport, bed texture, and channel planform at Mount Pinatubo, Philippines, *Earth Surf. Processes Landforms*, *37*, 1012–1022, doi:10.1002/esp.3241.
- Gran, K. B., D. R. Montgomery, and D. G. Sutherland (2006), Channel bed evolution and sediment transport under declining sand inputs, *Water Resour. Res.*, *42*, W10407, doi:10.1029/2005WR004306.
- Ham, D. G. (2005), Morphodynamics and sediment transport in a wandering gravel-bed channel: Fraser River, B.C. PhD thesis, 210 p., The Univ. of British Columbia, Vancouver B. C.
- Hickin, E. J. (1979), Concave-bank benches on the Squamish River, British Columbia, Canada, *Can. J. Earth Sci.*, *16*, 200–203.
- Howard, A. M. (1980), Thresholds in river regimes, in *Thresholds in Geomorphology*, edited by D. Coates and J. Vitek, pp. 227–258, Allen and Unwin, Boston.

- Iseya, F., and H. Ikeda (1987), Pulsations in bedload transport rates induced by a longitudinal sediment sorting: A flume study using sand and gravel mixtures, *Geogr. Ann., Series A, Phys. Geogr.*, *69*, 15–27, doi:10.2307/521363.
- Jackson, W. L., and R. L. Beschta (1984), Influences of increased sand delivery on the morphology of sand and gravel channels, *J. Am. Water Resour. Assoc.*, *20*, 527–533, doi:10.1111/j.1752-1688.1984.tb02835.x.
- Kleinhans, M. G. (2002), Sorting out sand and gravel: Sediment transport and deposition in sand-gravel bed rivers, PhD dissertation, Universiteit Utrecht, Utrecht, Netherlands.
- Knighton, D. A. (1999), The gravel-sand transition in a disturbed catchment, *Geomorphology*, *27*, 325–341.
- Kodama, Y. (1994), Downstream changes in the lithology and grain size of fluvial gravels, the Waterase River, Japan: Evidence of the role of abrasion in downstream fining, *J. Sediment. Res.*, *A64*, 68–75.
- Labbe, J. M., K. S. Hadley, A. K. Schipper, R. S. E. W. Leuven, and C. Peralta Gardiner (2011), Influence of bank materials, bed sediment, and riparian vegetation on channel form along a gravel-to-sand transition reach of the Upper Tualatin River, Oregon, *Geomorphology*, *125*, 374–382, doi:10.1016/j.geomorph.2010.10.013.
- Lamb, M. P., W. E. Dietrich, and J. G. Venditti (2008), Is the critical Shields stress for incipient sediment motion dependent on channel-bed slope?, *J. Geophys. Res.*, *113*, F02008, doi:10.1029/2007JF000831.
- Lopez, F., and M. Garcia (2001), Risk of sediment erosion and suspension in turbulent flows, *J. Hydraul. Eng.*, *127*, 231–235.
- McLaren, P., and P. Ren (1995), Sediment transport and its environmental implications in the Lower Fraser River and Fraser Delta, Canada Department of Environment, Environmental Conservation, Fraser River Action Plan, DOE FRAP 1995-03, 37 pp.
- McLean, D. G. (1990), Channel instability on lower Fraser River, PhD thesis, p. 290, The Univ. of British Columbia, Vancouver B. C.
- McLean, D. G., M. Church, and B. Tassone (1999), Sediment transport along lower Fraser River. 1. Measurements and hydraulic computations, *Water Resour. Res.*, *35*, 2533–2548, doi:10.1029/1999WR900101.
- Millar, R. G. (1999), Grain and form resistance in gravel-bed rivers, *J. Hydraul. Res.*, *37*, 303–312.
- Miller, M. C., I. N. McCave, and P. D. Komar (1977), Threshold of sediment motion under unidirectional currents, *Sedimentology*, *41*, 883–903.
- Nelson, P. A., W. E. Dietrich, and J. G. Venditti (2010), Bed topography and the development of forced bed surface patches, *J. Geophys. Res.*, *115*, F04024, doi:10.1029/2010JF001747.
- NHC (2006), Lower Fraser River hydraulic model final report, Report prepared for Fraser Basin Council, 61pp + tables, figures.
- NHC (2008), Comprehensive review of Fraser River at Hope, Flood hydrology and flows—Scoping study, Report prepared for British Columbia Ministry of Environment, 25pp + tables, figures.
- Nino, Y., and M. H. Garcia (1998), On Englund's analysis of turbulent energy and suspended load, *J. Hydraul. Eng.*, *124*, 480–483.
- Paola, C., and R. Seal (1995), Grain size patchiness as a cause of selective deposition and downstream fining, *Water Resour. Res.*, *31*, 1395–1407, doi:10.1029/94WR02975.
- Paola, C., G. Parker, R. Seal, S. K. Sinha, J. B. Southard, and P. R. Wilcock (1992), Downstream fining by selective deposition in a laboratory flume, *Science*, *258*, 1757–1760.
- Parker, G., and A. W. Peterson (1980), Bar resistance of gravel-bed streams, *J. Hydraul. Eng.*, *106*, 1559–1575.
- Parker, G., and Y. Cui (1998), The arrested gravel front: Stable gravel-sand transitions in rivers Part I—Simplified analytical solution, *J. Hydraul. Res.*, *36*, 75–100.
- Pickup, G. (1984), Geomorphology of tropical rivers. 1. Landforms, hydrology and sedimentation in the Fly and lower Purari, Papua New Guinea, *Catena Supplement*, *5*, 1–17.
- Rennie, C. D., and M. Church (2010), Mapping spatial distributions and uncertainty of water and sediment flux in a large gravel-bed river reach using an aDcp, *J. Geophys. Res.*, *115*, F03035, doi:10.1029/2009JF001556.
- Rice, S., and M. Church (1998), Grain size along two gravel-bed rivers: Statistical variation, spatial pattern and sedimentary links, *Earth Surf. Processes Landforms*, *23*, 345–365.
- Rust, B. R. (1978), A classification of alluvial channel systems, in *Fluvial Sedimentology, Mem. 5*, edited by A. D. Miall, pp. 187–198, Canadian Society of Petroleum Geologists, Calgary, Alberta.
- Sambrook Smith, G. H., and R. I. Ferguson (1995), The gravel-sand transition along river channels, *J. Sediment. Res.*, *A65*, 423–430.
- Sambrook Smith, G. H., and R. I. Ferguson (1996), The gravel-sand transition: Flume study of channel response to reduced slope, *Geomorphology*, *16*, 147–159.
- Shaw, J., and R. Kellerhals (1982), The composition of recent alluvial gravels in Alberta River beds, Alberta Research Council Bulletin, *41*, 151 p.
- Singer, M. B. (2008), Downstream patterns of bed material grain size in a large, lowland alluvial river subject to low sediment supply, *Water Resour. Res.*, *44*, W12202, doi:10.1029/2008WR007183.
- Singer, M. B. (2010), Transient response in longitudinal grain size to reduced gravel supply in a large river, *Geophys. Res. Lett.*, *37*, L18403, doi:10.1029/2010GL044381.
- Sternberg, H. (1875), Untersuchungen über Langen- und Querprofil geschiebeführender Flüsse, *Zeitschrift für Bauwesen*, *XXV*, 483–506.
- Venditti, J. G., W. E. Dietrich, P. A. Nelson, M. A. Wydzga, J. Fadde, and L. Sklar (2010), Mobilization of coarse surface layers in gravel-bedded rivers by finer gravel bed load, *Water Resour. Res.*, *46*, W07506, doi:10.1029/2009WR008329.
- Wiberg, P. L., and J. D. Smith (1987), Calculations of the critical shear stress for motion of uniform and heterogeneous sediments, *Water Resour. Res.*, *23*, 1471–1480, doi:10.1029/WR023i008p01471.
- Wilcock, P. R. (1998), Two-fraction model of initial sediment motion in gravel-bed rivers, *Science*, *280*, 410–412.
- Wilcock, P. R., and B. W. McArdeil (1993), Surface-based fractional transport rates: Mobilization threshold and partial transport of a sand-gravel sediment, *Water Resour. Res.*, *29*, 1297–1312, doi:10.1029/92WR02748.
- Wilcock, P. R., and B. W. McArdeil (1997), Partial transport of a sand/gravel sediment, *Water Resour. Res.*, *33*, 235–245, doi:10.1029/96WR02672.
- Wilcock, P. R., and J. C. Crowe (2003), A surface-based transport model for sand and gravel, *J. Hydraul. Eng.*, *129*(2), 120–128, doi:10.1061/(ASCE)0733-9429(2003)129:2(120).
- Wilcock, P. R., and S. T. Kenworthy (2002), A two-fraction model for the transport of sand/gravel mixtures, *Water Resour. Res.*, *38*(10), 1194, doi:10.1029/2001WR000684.
- Wilcock, P. R., S. T. Kenworthy, and J. C. Crowe (2001), Experimental study of the transport of mixed sand and gravel, *Water Resour. Res.*, *37*, 3349–3358, doi:10.1029/2001WR000683.
- Wolcott, J. (1988), Non-fluvial control of bimodal grain size distributions in river bed gravels, *J. Sediment. Petrol.*, *58*, 979–984.
- Yalin, M. S., and E. Karahan (1979), Inception of sediment transport, *J. Hydraul. Div., Am. Soc. Civ. Eng.*, *105*, 1433–1443.
- Yatsu, E. (1955), On the longitudinal profile of the graded river, *Eos Trans. AGU*, *36*, 655–663.
- Yatsu, E. (1957), On the discontinuity of grain size frequency distribution of fluvial deposits and its geomorphological significance, in *Proceedings of the International Geophysical Union Regional Conference*, pp. 224–237, Tokyo, Japan.